



University of
Stavanger

Faculty of Science and Technology

MASTER'S THESIS

Study program/ Specialization: Mechanical and Structural Engineering and Material Science/ Mechanical Engineering	Spring semester, 2013 Open
Writer: Vegard A. Brevik (Writer's signature)
Faculty supervisor: Hirpa G. Lemu	
Thesis title: Design, Analysis and Simulation of the Suspension System in the FS Team UiS Race Car	
Credits (ECTS): 30	
Key words: Suspension Stiffness Geometry Weight transfer	Pages: 56 + enclosure: 9 Stavanger, 1. July/2013 Date/year

Preface

Formula Student is a student competition where students shall design, build and compete with a one-seated formula-style racing car. The competition score is a combination of the cars performance on the track and the design, cost and business presentations held by the teams.

Formula Student Team UiS (FS Team UiS) represents the University of Stavanger in Formula Student and was founded in 2011 with the first participation in Formula Student in 2012.

This master thesis concerns the design and analysis of the suspension for the FS Team UiS car for Formula Student 2013.

Acknowledgements

I would like to thank Dr. Jan Kåre Bording, Tor Gulliksen and Jan Magne Nygård for assisting me with the many practical issues I encountered in the workshop. Fredrik Danielsen, Kjetil Kristiansen and Magne Øksnevad were a part of the 2012 FS Team UiS, I would like to thank them for aiding me with the design process. For performing the welding required when manufacturing the suspension system I want to thank Eirik Nesheim and Martin Bae. I would like to thank Dag Olav Gilje for machining several of the suspension components at the university workshop.

Since I have been very busy and had to spend a lot of time in the workshop I have had little time to discuss my design with my faculty supervisor, Hirpa G. Lemu, I would still like to thank him for his effort regarding administration of the Formula Student project at the university.

Innholdsfortegnelse

Preface.....	2
Acknowledgements	2
Abstract	5
Introduction.....	6
Suspension Theory	7
Key Terms and Concepts	7
Suspension Layout.....	10
Tire friction	10
Weight Distribution	10
Transverse Weight Distribution.....	10
Vertical Weight Distribution.....	11
Longitudinal Weight Distribution	12
Wheelbase.....	13
Track width	13
Aerodynamic effects.....	13
Virtual Race Track.....	14
Performance analysis	15
Suspension type	19
Suspension Geometry	21
Front view suspension geometry	21
Camber gain.....	21
Scrub.....	22
Jacking	24
Roll center	24
Front view suspension design	25
Weight Transfer.....	30
Longitudinal weight transfer	30
Transverse stiffness.....	33
Steering axis geometry.....	37
Load Analysis	42
Upright design	43
Pushrod design	46
Rocker design	49

ARB design.....	52
Conclusion	55
References.....	56
Appendix A – Virtual Racetrack Setup.....	57
Appendix B – Performance Analysis in Virtual Racetrack	61
Cornering.....	61
Braking.....	62
Acceleration.....	65
Distributing the Straight Length	65

Abstract

This master thesis concerns the design and analysis of the suspension for the Formula Student Team UiS racing car for the Formula Student 2013 student competition.

To analyze how parameters such as track width, wheelbase, weight distribution, CoG height and total weight affected the overall performance a virtual racetrack was constructed. Calculations were then done to find the cars lap time as the various parameters were altered.

Results showed that reduced weight and CoG height and increased track width and wheelbase all improved the performance of the car. The analysis do not incorporate the necessary weight increase to increase track width and wheelbase, thus, further calculations are needed to determine the full effect of changing these parameters. Nevertheless the rear track was increased from 1188 mm to 1240 mm to improve cornering ability.

The analysis revealed an increase in performance with increased rearwards weight distribution as high as 70/30 rear/front. This weight distribution causes the cornering ability to deteriorate but gave sufficient improvement for acceleration and braking to reduce the total lap time. The car was still designed with a 50/50 weight distribution due to all the complicating effects of reduced cornering ability such as over/understeer but this is a recommended area for further analysis.

Bump stiffness was designed based on required ground clearance during maximum acceleration. Since the track width is smaller than the wheelbase the car is inherently softer during lateral acceleration as opposed to longitudinal (e.g. braking) but the use of ARBs effectively increased the lateral stiffness (i.e. roll stiffness) without too much increase in bump stiffness. The use of adjustable ARBs also allows the roll stiffness and the sprung weight transfer distribution to be adjusted.

The suspension geometry was designed to minimize scrub and jacking while having good camber gain and roll center height. The camber gain front and rear is $0.0369^\circ/\text{mm}$ and $0.0426^\circ/\text{mm}$ respectively corresponding to a camber loss fraction of 0.58 and 0.54 respectively. The roll center front and rear is 58.3 mm and 61 mm above the ground respectively. This height ensures that jacking and scrub are kept low while there is a large roll moment giving a large amount of sprung weight transfer which can be distributed between the front and rear track depending on chosen ARB stiffness's.

Introduction

This master thesis concerns the design and analysis of the suspension system on the 2013 FS Team UiS car. All components of the suspension have been designed as part of this thesis with the exception of: rims, tires, hubs with bearings and components which are part of the steering system. The design of steering system components concern another master thesis and will therefore not be described here. Rims, tires and hubs are described in this thesis but not designed or analyzed since these are taken from the FS Team UiS 2012 car due to economic reasons. The design process is however only shown for some selected components, the rest are shown in assembly drawings.

The main focus of this thesis is on the geometry and stiffness of the suspension and its effect on the overall performance of the car.

Suspension Theory

In this master thesis the term suspension refers to all components connecting the frame of the car to the wheels with the exception of the drivetrain and the steering system. The position of the wheels (i.e. wheelbase and track width) will not be referred to as part of the suspension but will be designed/chosen and analyzed in this thesis.

The requirements of the suspension system on a racing car are:

- To connect the frame of the car to the wheels with sufficient strength to withstand all anticipated loading situations.
- To absorb motions between the car and the road in such a manner that no part of the car is damaged. This demands that the suspension system is soft enough to allow motion between the car and wheels and stiff enough to avoid undesirable contact between the car and the road.
- To dissipate undesirable motion between the car and the road. This is usually achieved with viscous dampers in the suspension system.
- To reduce the negative effects of weight transfer during handling situations such as braking, cornering and acceleration.
- To ensure optimal tire angles with the road for various handling situations.
- To be as light weight as possible, especially concerning the unsprung and rotational weight.
- Facilitate desired weight distribution for the wheels

Key Terms and Concepts

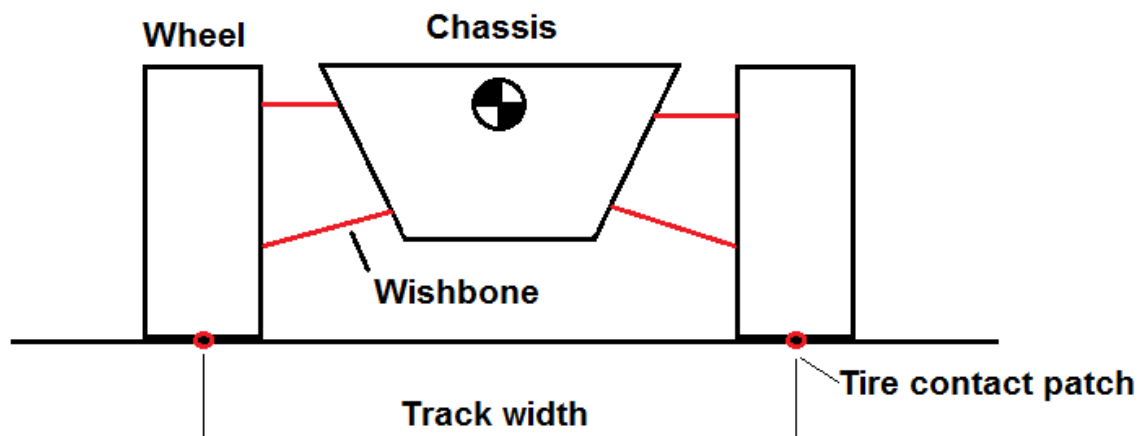


Figure 1. Front view of car

- Tire contact patch is the area which the tire is in contact with the ground
- Track width is the distance between the centers of the tire contact patch in the transverse direction. If track width is different front and rear the mean track width is:

	$\frac{\text{Track front} * \text{weight front} + \text{track rear} * \text{weight rear}}{\text{Total weight}}$	

- The angle between the wheel and the vertical axis is called the camber angle and is defined as negative when the wheels are tilted towards the chassis at the top. Despite this convention it is referred to as camber gain when a wheels camber becomes negative with an upwards motion of the wheel relative to chassis. Camber is an important concept because it largely determines the wheels grip.
- Weight transfer during acceleration of the car is given by the equation:

	$\text{Weight transfer} = \frac{M * A * H}{L}$	
--	------------------------------------------------	--

Where M is the mass of the car, A the acceleration, H is the height to the center of gravity (CoG) and L is the distance between the center of the wheels in the direction of the acceleration. For lateral acceleration for example L would be the track width.

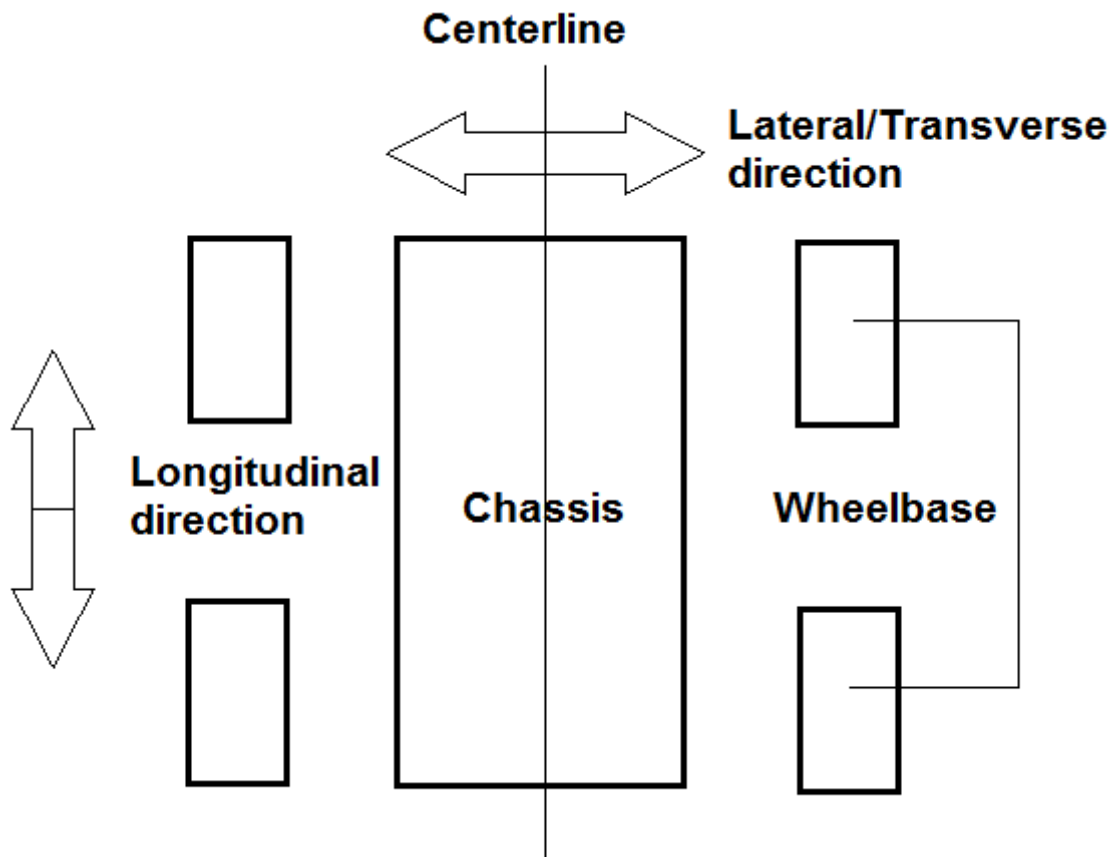


Figure 2. Top view of car

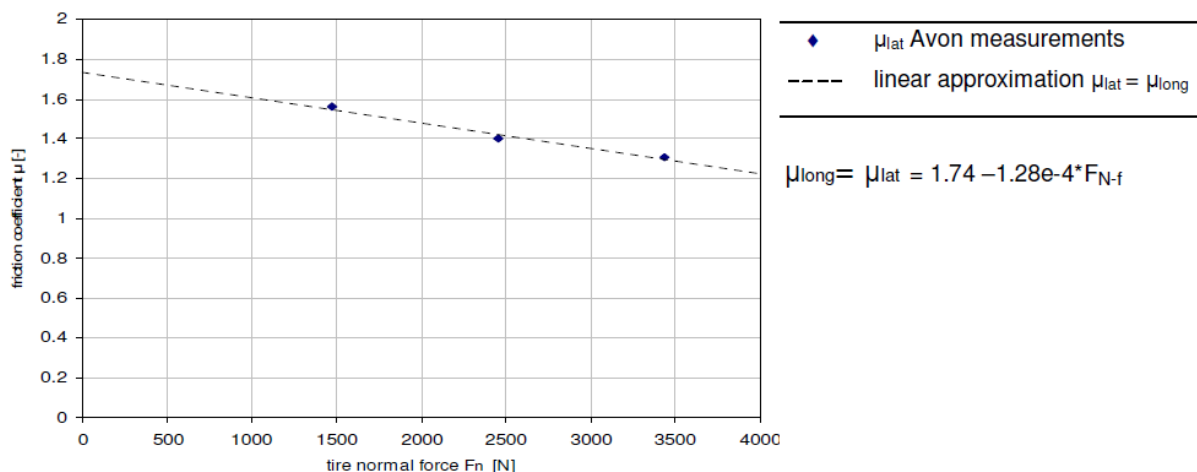
- Wheelbase is the distance between the centers of tire contact patch in the longitudinal direction.
- The angle between a wheel and the centerline is called the toe angle, or simply, toe. It is referred to as toe-in when the front side of the wheel tilts towards the centerline. Toe angle has not been analyzed in this thesis since it can be adjusted later based on tire wear.

Suspension Layout

In this thesis the term suspension layout covers the general placement and setup of the suspension components and the wheelbase and track widths of the car. Mass distribution will also be covered in suspension layout since the positioning of the wheels determines the mass distribution relative to the wheels.

Tire friction

Test data for the 20.5x7.0-13 Hoosier road racing slicks which will be used on the FS Team UiS 2013 car are not available, therefore estimated coefficients of friction based on test data for the 20.0x7.0-13 Avon 3 ply pro-series will be used. These tires are very similar in size with the same tread width and they are both bias racing slicks frequently used for Formula Student/FSAE. Avon provides testing data for this tire at a camber angle of 2° and a pressure of 20 psi (1.38 bars). The coefficients of friction has been derived from this test data in the master thesis Chassis and suspension design FSRT02 by A. van Berkum (2006) at the Technical University of Eindhoven and is summarized in the figure below.



Figur 3. Tire friction coefficient vs tire normal load. From Chassis and Suspension Design FSRT02 by A. van Berkum (2006)

The figure above shows the load sensitivity of the tire, that is, how the coefficient of friction is reduced with increasing load. Also note that the coefficient of friction is the same in both the lateral and longitudinal direction.

Weight Distribution

Transverse Weight Distribution

For a race car which travels on a track with turns in only one direction, such as NASCAR, it can be an advantage to place the CoG away from the centerline. This is because the car doesn't need to have the same cornering abilities in both directions. In Formula Student the race track varies with right and left turns which the car should handle as equally as possible. Therefore the CoG should be on the centerline of the car and the suspension should be symmetric about the centerline.

Vertical Weight Distribution

With a given wheelbase, track width and acceleration the vertical position of the CoG determines the weight transfer between the front and rear and the left and right side. Increasing the height of the CoG increases the weight transfer proportionally. For cornering and braking the weight transfer is undesirable due to load sensitivity of the tires and because it causes roll and dive. Roll and dive can reduce the performance of the car because it can alter the tires alignment with the road and it requires a certain stiffness of the suspension. When the weight is transferred from one side to the other because of cornering or braking the load sensitivity of the tires causes the coefficient of friction of the tires on the heavily loaded side to be reduced and the coefficient of friction on the light side to increase. The total grip of the car is reduced by this effect which in turn reduces the cars cornering and braking ability.

For a car with rear wheel drive the weight transfer during acceleration will usually be beneficial since it increases the load on the rear wheels which increases the grip and thus increases the acceleration. Since the engine power is limited the amount of grip necessary for maximum acceleration decreases with increasing speed. This is not the case for cornering and braking where grip is the limiting factor regardless of the speed. Because available grip for a race car usually is only an issue at low speeds and when starting the CoG is commonly placed as low as possible because it reduces the disadvantages of weight transfer concerning cornering and braking.

The CoG height for the 2012 FS Team UiS car was never measured and it is difficult to predict the CoG height for the 2013 car since it is currently being designed. The total weight of the 2012 car was 258 kg. The weight of the unsprung components has been listed below.

Table 1. Weight of unsprung components

Component	Weight
Lower wishbone*	605 g
Upper wishbone*	481 g
Drive axle*	846 g
Axle bearing and housing	667 g
Upright	811 g
Upright brackets w/fasteners	310 g
Hub (Aluminium)	266 g
Brake disc	491 g
Brake caliper +fasteners and bracket (front)	710 g
Brake caliper +fasteners and bracket (rear)	510 g
Wheel	8262 g
Pushrod*	352 g
Tie-rod*	350 g
Toe-rod*	248 g
Unsprung weight rear	24634 g
Unsprung weight front	22956 g
Total unsprung weight	47590 g

* indicates partially unsprung components for which half the weight is assumed to be unsprung.

The unsprung weight is approximately centered about the center of the wheel in longitudinal and vertical direction. The wheels have an outer diameter of 20.5 inches giving the unsprung weight a CoG height of 260.35 mm above the ground.

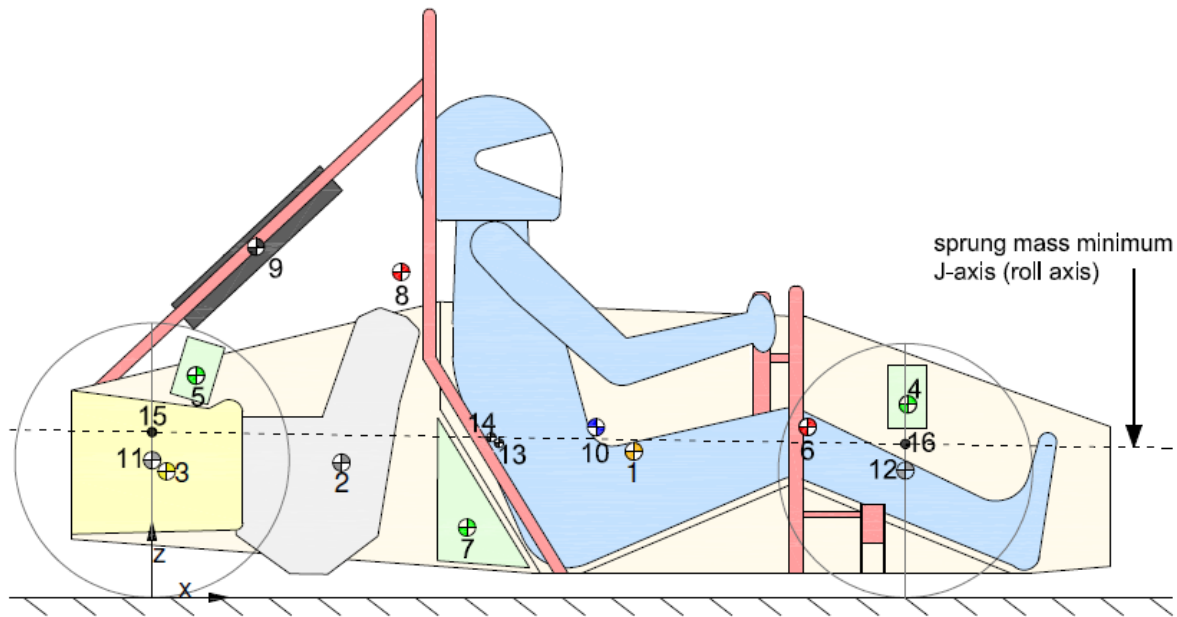


Figure 4. Weight distribution on a race car. From Chassis and Suspension Design FSRT02 by A. van Berkum (2006)

In the figure above the CoG for the chassis is 300 mm above the ground and the CoG for the sprung mass including the driver is 329 mm above the ground. The designed 2013 car frame has a CoG height of 354 mm above ground (based on estimates by frame designer Eirik Nesheim and body designer Adrian Fagerlund). The FSRT02 car has a sprung weight CoG 29 mm above the frame CoG, by assuming the 2013 car have a similar weight distribution relative to the frame the sprung weight CoG is: $354 \text{ mm} + 29 \text{ mm} = 383 \text{ mm}$. To be conservative the CoG height is rounded up to 400 mm above the ground.

The 2013 car has a design total weight of 250 kg and a 100 kg driver will be assumed in this thesis.

Table 2. Estimated vertical weight distribution.

	Mass [kg]	Height CoG from ground [mm]
Sprung weight w/driver	302,4	400
Unsprung weight	47,6	260
Total weight	350	381

Longitudinal Weight Distribution

The longitudinal position of the CoG can be used to increase the grip during acceleration by placing it rearwards. For a car where the front and rear tires are equal a rearward mass distribution can also increase the braking grip as it can compensate for some of the weight transfer. When it comes to cornering the effect of the longitudinal position of the CoG is more complicated due to the number of variables and because corner entry and exit situations can have a significant effect on the cars performance. The variables which complicate cornering analysis are track width, suspension stiffness, roll center and tire sizes which can all be different from the front to the rear.

Wheelbase

For a given CoG height and longitudinal acceleration the wheelbase determines the longitudinal weight transfer and thus affect the required stiffness and strength of the suspension. A long wheelbase reduces the weight transfer which can allow a softer suspension with lighter components, can increase braking ability and improve straight line stability. Negative effects of a long wheelbase is reduced weight transfer during acceleration which improves acceleration grip, increased chassis weight due to longer span between the wheels, increased cornering radius and angular inertia.

The FS Team UiS 2012 car had a wheelbase of 1620 mm.

Track width

The track width affects the transverse load transfer and stiffness similarly to how the wheelbase affects the longitudinal load transfer and stiffness, the main difference being that it is common to separately adjust the transverse stiffness using anti roll bars (ARBs) and that transverse load transfer has only negative effects.

The FS Team UiS 2012 car had a front and rear track width of 1288 and 1178 mm respectively giving a mean track of 1233 mm with a 50/50 weight distribution.

Aerodynamic effects

The downforce from the aerodynamic devices is based on a CFD analysis in Autodesk Inventor Professional of the entire car. The result was a downforce of 622 N at a speed of 60 km/h. Since downforce is the same as lift only in the opposite direction the same formula can be used:

$$DF = L = \frac{1}{2}\rho AC_L v^2$$

Where DF is downforce in newton, L is lift in newton, ρ is the density of air in kg/m^3 , v is velocity in m/s, A is the planform area in m^2 and C_L is the lift coefficient at a given angle of attack, Mach-number and Reynolds number.

If we neglect the changes of the lift coefficient we can simplify this equation to:

$$DF = K_{DF} v^2$$

With the downforce and velocity from the CFD analysis $K_{DF} = 2.239 \text{ kg/m}$. This simple equation can then be easily used to approximate the downforce for different speeds. The design of the aerodynamic devices is not completed and a CFD analysis might be different from actual results, therefore the amount of downforce actually achieved might be different than the one calculated in this thesis. Nevertheless it is necessary to have some rough estimate when designing the suspension. The combined effect of the aerodynamic devices is assumed to act as a resulting force in the middle of the front and rear wheels.

CFD analysis revealed a drag of 471 N at 60 km/h. The same equation can be used for drag as for downforce giving a $K_{DRAG} = 1.6963 \text{ kg/m}$.

Virtual Race Track

To illustrate how the car's performance during braking, cornering and acceleration affect the overall performance, e.g. lap time, a virtual racetrack has been constructed. Since it is not possible to know how the actual racetrack at Silverstone will be and it is mathematically complicated to model such a racetrack a simplified oval racetrack has been constructed where the radius of the corners and the length of the straights have been based on the FSAE 2013 guidelines for design average and top speeds of the racetrack and simplified performance calculations for a Formula Student race car. The detailed calculations for the racetrack can be found in appendix A.

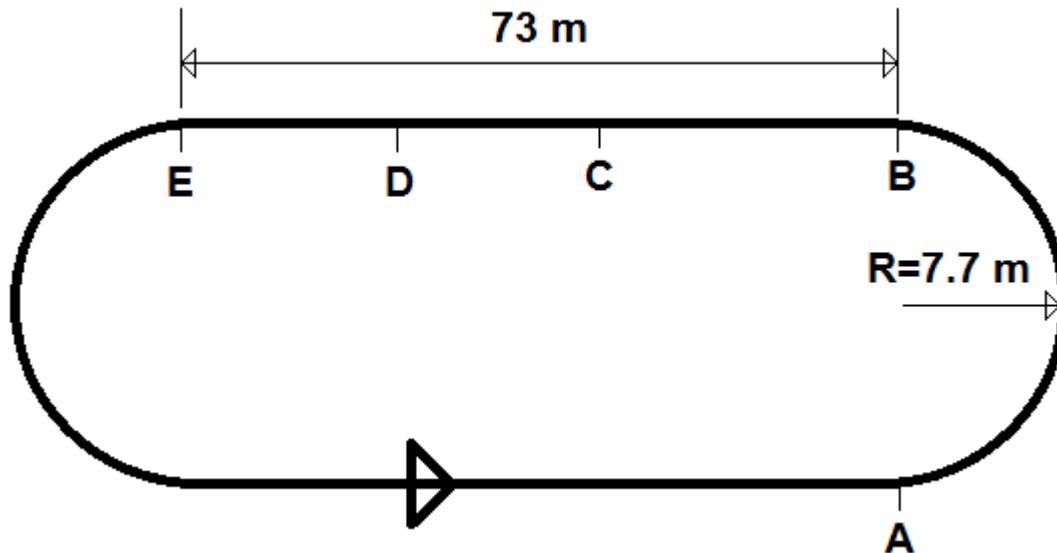


Figure 5. Dimensions for virtual racetrack

In the figure of the oval racetrack the letters signify the following:

A: Corner entry, B: Corner exit and grip-limited acceleration, C: Power-limited acceleration, D: Braking (speed reduction before cornering), E: Corner entry.

Both the calculations for construction of the virtual racetrack and the calculations done to evaluate a race car on the virtual racetrack will be based on the following assumptions:

- The car will always be accelerating, either laterally (i.e. cornering) or longitudinally (i.e. braking or increasing speed), at its limit but will never do more than one at the same time, e.g. accelerating out of a corner is neglected.
- Engine power is 59.6 kW (80 hp) constantly when applied.
- The corners are driven as a constant radius turn with constant speed.
- Braking reduces the speed to exactly the maximum speed possible to complete the corner.

Performance analysis

Table 3. Input values for performance analysis

Weight	Wheelbase	Mean Track	Height CoG	Fraction front weight
350 kg	1600 mm	1265 mm	381 mm	0.5

Calculations for performance analysis are shown in appendix B.

Table 4. Lap times for various car weights

Weight [kg]	Lap time [s]
320	11.14
330	11.22
340	11.29
350	11.36
360	11.43
370	11.50
380	11.57

Table 4 has been included to quantify the performance loss for added weight on the car. By taking the 350 – 360 kg interval and assuming a linear relationship the percent increase in lap time per kg added weight can be calculated:

	$\frac{11.43 - 11.36}{11.36} * 100 \% = 0.6162 \%$	
	$\frac{0.6162 \%}{360 \text{ kg} - 350 \text{ kg}} = 0.062 \%/\text{kg}$	

For the virtual race track the increase in lap time and thus decrease in performance is 0.062 %/kg of added weight.

Table 5. Lap times for different CoG heights

Height CoG [mm]	Lap time [s]
200	11.02
250	11.11
300	11.20
350	11.30
381	11.36
400	11.40

As previously mentioned the only benefit from an increased CoG height is the rearwards weight transfer during acceleration which increases the grip. For the virtual racetrack the increased acceleration grip does not compensate for the performance loss in cornering and braking resulting in

increased lap times for increased CoG height. It should be noted that for a racetrack with lower corner exit speeds the lap time versus CoG height characteristics could be different.

A low CoG height also reduces the required weight and stiffness of the suspension/chassis since maximum loads are lower. These effects have not been included in the calculations for table 5 and will increase the overall benefits of a low CoG.

Best overall performance with a low CoG is an expected result as it is a common design goal for racing cars, nevertheless, it is difficult to place the CoG low due to ground clearance requirements, large components such as engine and driver and space requirements for the driver within the chassis.

Table 6. Lap times for different wheelbases

Wheelbase [mm]	Lap time [s]
1300	11.44
1400	11.41
1500	11.38
1600	11.36
1700	11.34
1800	11.32
1900	11.31

Wheelbase must be minimum 1525 mm, lower entries shown for illustration purposes only.

Increased wheelbase increases braking while decreased wheelbase increases acceleration grip. Table 6 shows that for the virtual racetrack the benefits of increasing the wheelbase outweigh the negative effects. This might seem strange but increased braking capabilities allow more time for acceleration/high speeds before speed reduction for corner entry is required, nevertheless, the results in table 6 are very track dependent and the time and distance with grip-limited acceleration are very small due to high corner exit speed on this track.

A larger wheelbase increases the span between the load points (i.e. wheels) resulting in larger loads on the chassis while weight transfer is reduced which reduces the maximum load on the suspension. The result is a heavier chassis to meet the strength and stiffness requirements and a lighter suspension. Since the chassis is the larger and heavier component it can be assumed that an increase in wheelbase will result in an overall increase in weight. Cornering inertia, cornering radius and cornering space requirements also increase with the wheelbase.

The wheelbase will be set to 1600 mm due to all the effects which are difficult to quantify and have not been taken into account in table 6 since these outweigh the small theoretical benefits of increasing the wheelbase based on a qualitative assessment. The FS Team Uis 2012 car has a wheelbase of 1620 mm.

Table 7. Lap times for various mean tracks

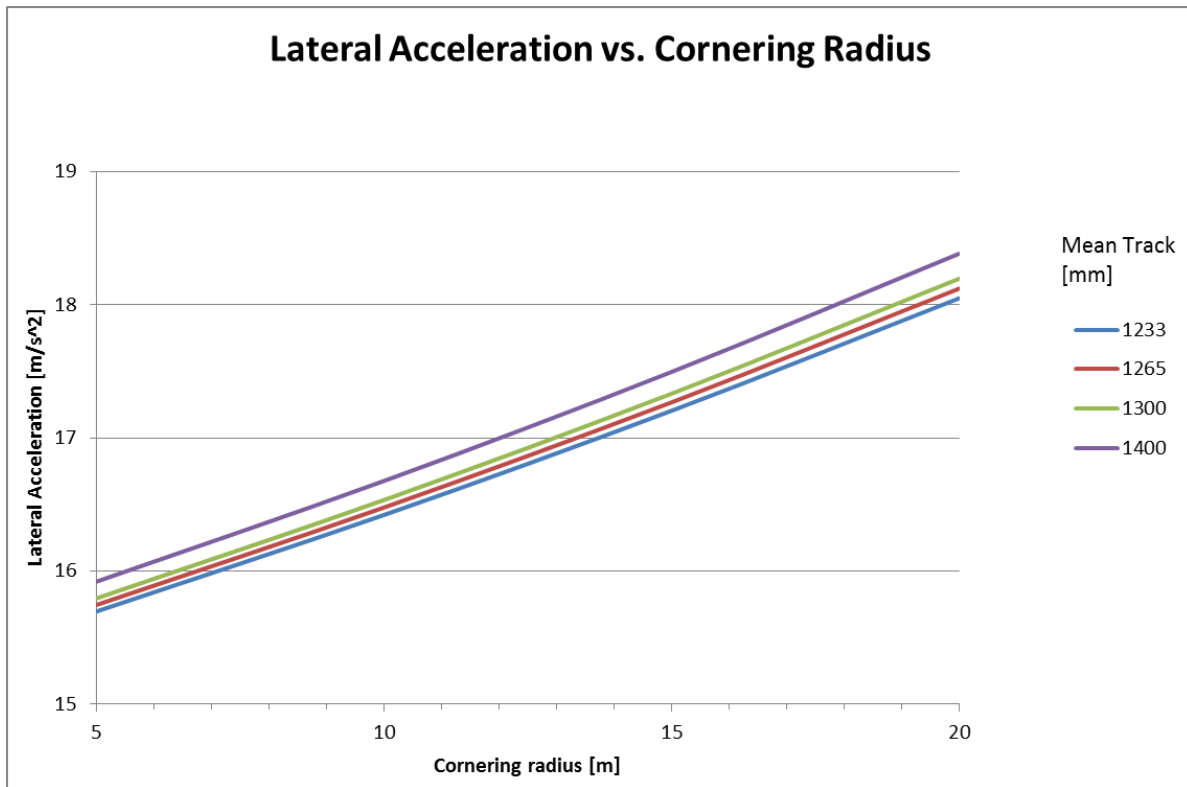
Mean track [mm]	Lap time [s]
1200	11.37
1233	11.36
1245	11.35
1300	11.34
1400	11.32
1500	11.29
1600	11.28
1700	11.26

In the lap time calculations the mean track only affects the cornering speed and increasing the mean track will only yield beneficial effects. Regarding actual performance increasing the mean track will add weight since longer wishbones are needed and available space in the track will be less since the car will be wider. According to FSAE 2013 rules the minimum track width for the racetrack is 4.5 m and the edges are covered in cones. A penalty time is awarded the team for each cone which is hit. A vehicle with a smaller track is thus easier to maneuver around the track and can drive through corners along a more beneficial track.

From table 7 we see that increasing the mean track from 1100 to 1700 mm results in a 1.3 % reduction in lap time. Though this is a significant improvement the added weight and width of the vehicle would also be significant for a 600 mm increase in track width.

The FS Team UiS 2012 car had a larger track front than rear, this was done to have improved maneuverability in tight corners and because it is desirable for the front wheels to take most of the cornering weight transfer allowing the rear wheels more grip for acceleration out of a corner. Based on table 7 above increasing the mean track should be beneficial but it is not desirable to increase the front track significantly because it would increase the space needed on a racetrack which can have some narrow portions.

The front track will be increased from 1288 to 1290 mm and the rear track will be increased from 1188 to 1240 mm giving a mean track of 1265 mm.



Figur 6. Plot of max lateral acceleration vs cornering radius

Tabell 8. Cornering speeds and lap times for different longitudinal weight distributions

Fraction weight front	Lap time [s]	Cornering speed [m/s]
0.2	11.26	10.88
0.3	11.18	10.96
0.4	11.29	11.04
0.5	11.36	11.13
0.6	11.50	11.04
0.7	11.60	10.96
0.8	11.68	10.88

Table 8 shows that the best lap time is achieved with a car having a weight distribution around 30/70 front to rear. As mentioned in longitudinal weight distribution a rearwards CoG can improve both braking and acceleration while its effect on cornering is more complicated. The calculations in table 8 assume equal front and rear roll stiffness resulting in equal load transfers front and rear and the only difference in tire load is the longitudinal weight distribution. For such a case we notice that the highest cornering speed is obtained at a 50/50 weight distribution and that the cornering speed is symmetric about this weight distribution, e.g. a 70/30 and 30/70 front to rear weight yields the same cornering speed.

Though table 8 indicates a significant performance improvement with a rearwards CoG the race car will still be designed for a 50/50 weight distribution because:

- A rearwards CoG can cause excessive oversteer which makes the car more difficult to handle for the driver during cornering
- It is difficult at this time in the design process to make such a significant change in the suspension layout as it affects the design of other systems.
- A rearward CoG will decrease the mean track width when the rear track is smaller

Suspension type

For a race car the most common suspension types are the MacPherson strut and the double wishbone (also commonly referred to as double a-arm and short-long arm (SLA) when the wishbones are of unequal length).



Figure 7. MacPherson strut. From www.team-inegra.com

The MacPherson strut is the simplest of the two suspension types and requires the least amount of bearings making it the cheapest alternative. It also has plenty of space for the drive axle to connect to the hub. For commercial cars the MacPherson strut is easy to use since the chassis builds around the wheel. In the Formula Student competition the rules dictate that the wheels shall be clearly visible when the car is seen from above meaning that the chassis cannot cover the top of the wheels making the MacPherson strut difficult to use, especially on the rear of the car where the chassis is very low. There is also little camber gain during vertical movement for a MacPherson Strut which is undesirable in racing.

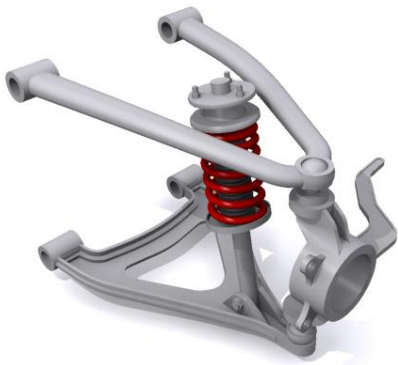


Figure 8. Double wishbone. From www.carbibles.com

The double wishbone suspension allows better control of roll center and camber gain and is easily fitted on an open wheel vehicle.

The double wishbone suspension with a longer lower than upper wishbone was used on the 2012 car and will also be used on the 2013 car. The unequal wishbone length gives camber gain in bump and fits the chassis design which is narrow at the bottom and wider at the middle to ensure enough space for the engine in the rear and the driver in the front.

Since it is economically desirable to use the dampers from the 2012 car and these have a length of only 200 mm a pushrod will be connected to the lower wishbone and a rocker, the damper will then be connected between the rocker and the chassis. The use of a rocker adds a component to the system but allows the motion ratio between the wheel and the damper to be adjusted and can be used as a pick-up point for the ARB system.

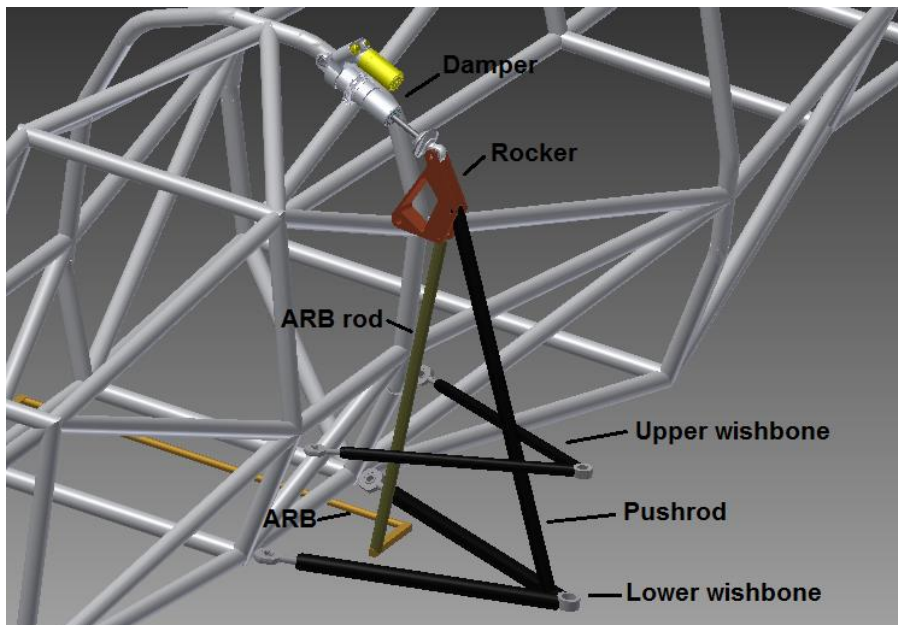


Figure 9. Showing the suspension setup in this thesis

Suspension Geometry

In this thesis the term suspension geometry covers the geometry consisting of the wishbones' connection points towards the frame and upright. The suspension geometry can be divided into front view and side view geometry.

Front view suspension geometry

There are four important effects which should be considered when designing the front view suspension geometry; jacking, scrub, camber gain and roll center position.

Camber gain

When a car rolls during cornering the outer wheel will rise relative to the chassis (bump) while the inner wheel will fall relative to the chassis (droop). If the wheels maintain the same angle relative to the chassis with vertical movement chassis roll will change the wheels alignment with the ground which reduces the grip. To avoid or reduce the misalignment of the wheels during cornering the suspension can be designed to give increasingly negative camber in bump and eventually increasingly positive camber in droop. Positive camber gain in droop is less important since the load on the inner wheel during cornering is reduced.

To determine the camber gain for a double wishbone suspension extend the lines of the wishbones in front view until they intersect. The intersection point is the instant center (IC) of the suspension mechanism and the horizontal distance between the upright pivot axis and the IC is the front view swing axle (FVSA). Since the track widths have been designed but not the upright and hub the center of the tire contact patch will be used instead of the upright pivot axis, the difference is the same as the scrub radius and is neglectable. The IC allows us to view the double wishbone suspension as if the wheel was mounted on a solid axle which simplifies visualization and calculations. Note that the IC will change as the suspension moves and thus only gives exact values for the instantaneous motion.

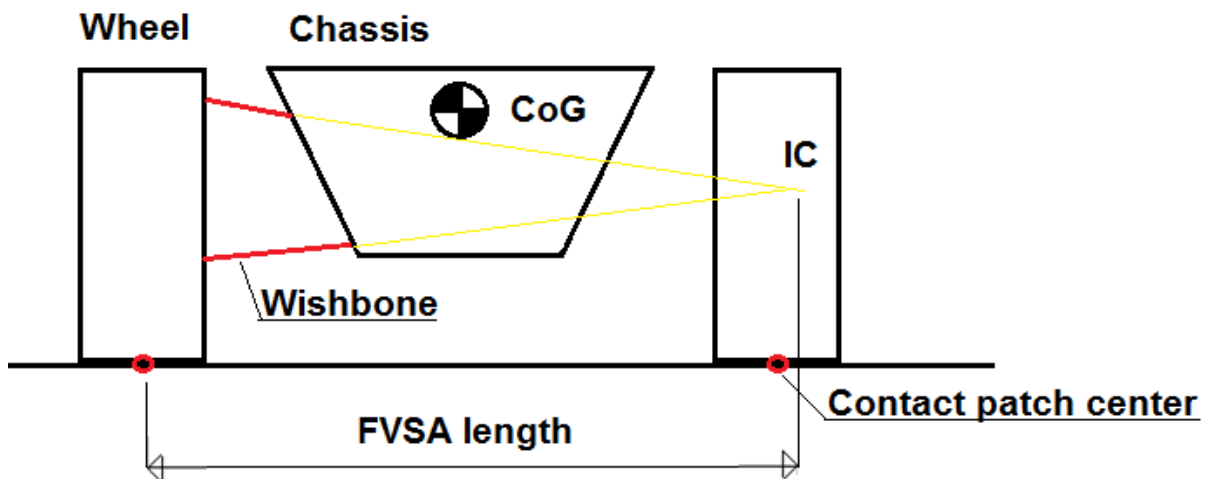


Figure 10. Showing front view geometry with IC

Once the FVSA length has been found the corresponding camber gain (CG) is given by:

	$CG = \arctan(1/FVSA \text{ length})$	
--	---------------------------------------	--

Where FVSA length is given in mm and CG in °/mm

To effectively design for a certain camber gain the camber loss in roll must be determined.

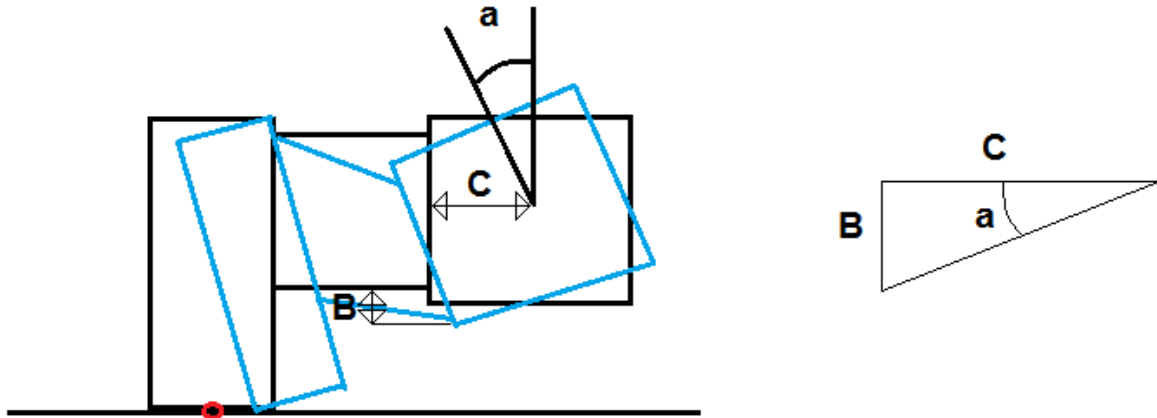


Figure 11. Showing wheel travel as a result of chassis roll

The figure above shows how a chassis roll angle α causes a wheel travel of B relative to the chassis for a double wishbone suspension with parallel and equal wishbones meaning that there is no camber gain with vertical wheel motion. Notice that the angle between the wheel and chassis is unaltered giving the wheel the same angle α relative to the ground as the chassis. C is the distance from the chassis center to the connection point of the lower wishbone on the upright, i.e. half the track width assuming no scrub.

	$\tan \alpha = B/C$	
For small angles, we can approximate:	$\alpha = B/C$	
	$\alpha/B = 1 \text{ rad}/C$	
Converting radians to degrees:	$\alpha/B = 57.296 \text{ }^\circ/C = CL$	

With C in mm we get the camber loss (CL) in °/mm.

For the front and rear track C is 645 and 620 mm respectively giving a front CL = 0.0888 °/mm and a rear CL of 0.0924 °/mm.

Scrub

Since a wheel rotates about a certain IC in bump and droop a lateral motion relative to the chassis can occur, this is called scrub and is an undesirable effect since it can induce lateral motion of the car and changes the track width.

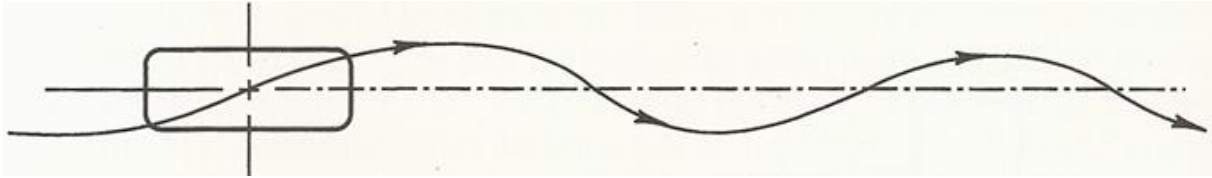


Figure 12. From www.motortrike.com/TrikeIRSfacts.aspx

The figure above shows the wheel path on a rough road for a wheel with excessive scrub. The vertical disturbances in the road cause a lateral disturbance in the wheel path.

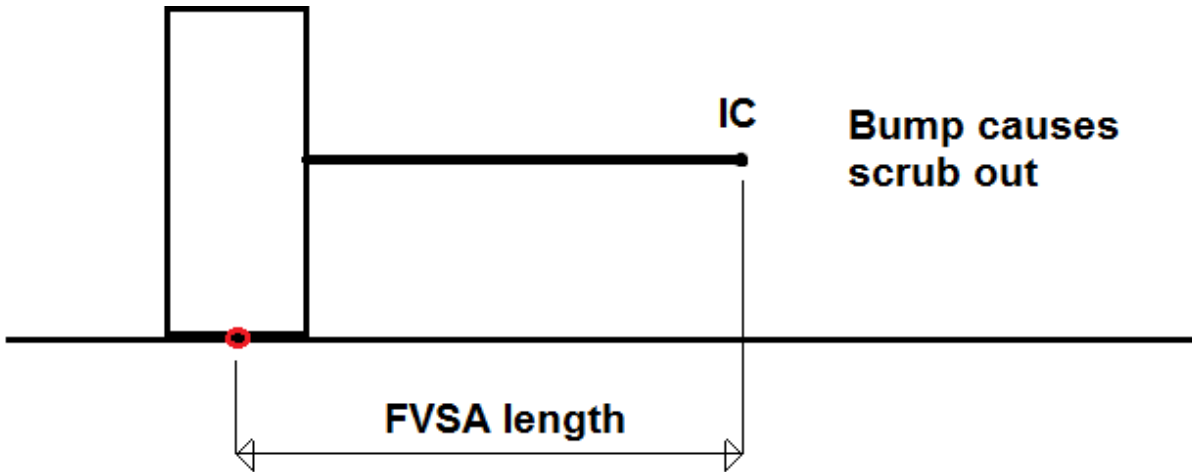


Figure 13. High IC

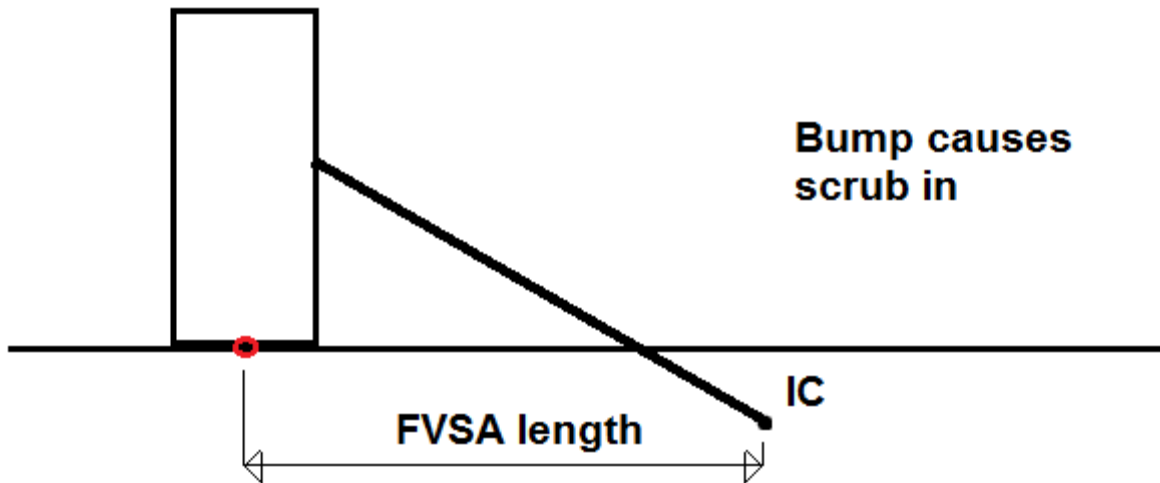


Figure 14. IC below ground

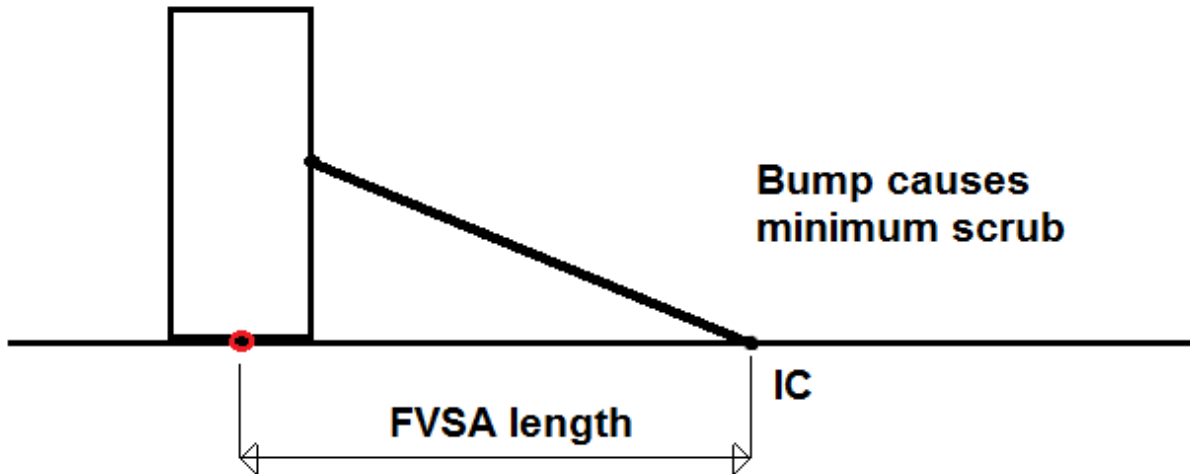


Figure 15. IC on the ground

The figures above show how the scrub is affected by the height of the IC above ground. Minimum scrub is achieved by placing the IC on the ground. Increasing the FVSA will also decrease the scrub.

Jacking

During cornering the lateral forces which act on the tire contact patch generate a moment about the IC of the wheel. If the IC is above ground the force will push the sprung mass up and if the IC is below ground the force will push the sprung mass down, both effects are called jacking. An IC on the ground eliminates jacking but as mentioned the IC will change with suspension motion and an attempt to place the IC on the ground can cause the IC to move through the ground which yields erratic handling behavior.

Roll center

The front view suspension geometry contributes to the cars reaction to lateral acceleration since it determines the roll center (RC) which the chassis will roll around. The RC can be kinematically determined by extending lines from the IC and the center the tire contact patch. Doing this for both sides of the suspension gives two lines, the intersection point of these two lines is the RC.

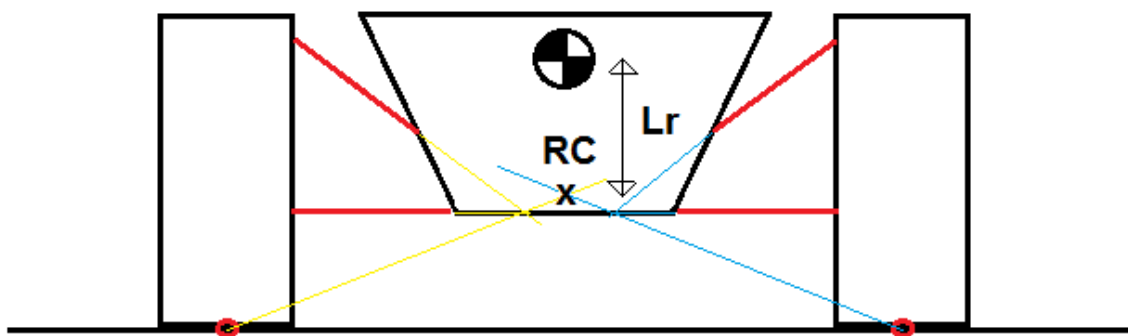


Figure 16. Illustration of roll center

The height of the RC determines how much of the cornering weight transfer is transferred through the springs and how much is transferred through the wishbones. If the RC is positioned at the CoG all lateral weight transfer goes through the wishbones which means that lateral acceleration does not induce chassis roll. A RC over or under the CoG will make the chassis lean into or out of the corner respectively. The chassis roll moment is given by the lateral force and the vertical distance, L_r , between the RC and the CoG. If all other suspension parameters are given the body roll will thus vary linearly with L_r .

The obvious benefit of placing the roll center close to the CoG is the reduced chassis roll during cornering. Note that the weight transfer is the same regardless of the RC position, the RC position only determines the load path for this load transfer. The advantage of placing the RC further away from the CoG is that we can determine how the weight transfer is distributed between the front and rear track. The track with the highest roll stiffness will take the largest amount of weight transfer resulting in less weight transfer for the softer track. The roll stiffness of the tracks can be adjustable by fitting adjustable ARBs, this allows us to adjust the weight transfer after the car has been built which means that the over/under steer characteristics of the car will be adjustable. With a small L_r this adjustability is reduced.

It is undesirable to allow the RC to move through the CoG since this will change the roll direction causing erratic handling.

Front view suspension design

As can be seen from the previous sections the suspension design is based on trade-offs as it is impossible to alter one trait without affecting another. For example; a long FVSA is beneficial for reducing scrub but will limit the amount of camber gain and a high roll center will reduce roll but requires a high IC which results in large jacking moments.

The design goals will be prioritized as shown below:

- Reducing camber loss due to chassis roll to half of CL
- Placing the RC roughly 80 mm above ground

Reducing the camber loss improves the cornering grip but reduces the grip during braking and acceleration since the longitudinal weight transfer will push the suspension down without rolling the chassis. So the designed camber gain in roll becomes camber loss in acceleration induced squat and braking induced dive.

A RC 80 mm above ground ensures enough weight transfer through the springs to be distributed between the front and rear track while ensuring that the jacking will not change direction due to IC migration through the ground.

Based on the body design the height from the ground to the bottom of the chassis tubes should be 126 mm at the position of the front and rear suspension when the chassis is horizontally oriented. The use of pushrods will make the height adjustable but 126 mm will be used as the design value. The wheel outer diameter is 530 mm and the available space within the upright limit any wishbone connection points to 110 mm from center. To limit the amount of different parts required the uprights will be made symmetric to allow the same design to be used on both sides. This requires the upper and lower wishbones to have connection points at the same distance from the wheel center.

To achieve camber gain the FVSA length must be short, i.e. the IC must be close to the wheel which can be achieved by assuring that the wishbone connection points are further apart on the upright than on the chassis. Therefore the upright connection points are preliminary set at maximum distance from the wheel center. To avoid a high IC the lower wishbone should point horizontally or slightly downwards towards the chassis. Since the design height has been set the lower wishbone will be placed at the lowest possible point on the chassis.

For the front the following is then given:

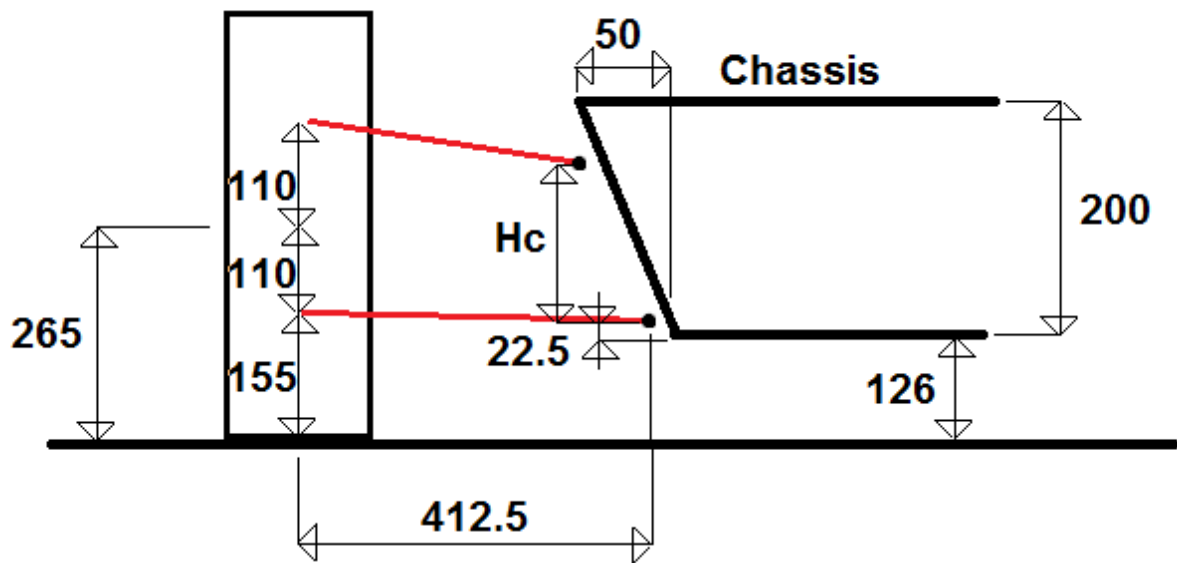


Figure 17. Showing front view geometry for the front suspension

The IC and RC can be found both graphically and mathematically. Graphically tends to be imprecise, mathematically is time consuming but by setting up the variables in an excel sheet the variables can be easily changed to design the right IC/RC and it can also be used for different wheel travel.

We want to express the lines on the form:	$y = ax + b$	
For start and end coordinates x_s, y_s and x_e, y_e respectively:	$a = (y_e - y_s)/(x_e - x_s)$	
To determine constant b:	$b = y_e - a*x_e$	

With expressions for the upper and lower wishbone lines defined as y_U and y_L respectively the intersection point can be found:

	$y_U = y_L$	
	$a_U*x_{IC} + b_U = a_L*x_{IC} + b_L$	
	$x_{IC} = (b_L - b_U)/(a_U - a_L)$	
The IC y-coordinate is found by inserting x_{IC} into the expression for either y_U or y_L	$y_{IC} = a_U*x_{IC} + b_U$	

The same process is done for the line between the tire contact patch and IC. The process is then repeated for the other side of the suspension and the intersection point which constitutes the RC is found. It requires some manual iteration to find a suitable IC and RC. To reduce the workload L_5 is kept constant while in reality it would change slightly with L_2 because of the angled tube on the chassis which the upper wishbone is connected to.

Table 9. Input for front suspension geometry

Input								
$\Delta y^{(1)}$	L1	L2 ⁽²⁾	L3	L4	L5	L6	L7	L8
6.5	412.5	170	220	362.5	50	155	0	232.5

⁽¹⁾ Since the geometry was setup with an initially horizontal lower wishbone Δy was set to the value which gives the correct ground clearance according to figure 16. $155 - 126 - 22.5 = 6.5$

⁽²⁾ L_2 has been adjusted to find suitable IC and RC

Table 10. Output for front suspension geometry

Output							
α	$\beta + \gamma$	ICx Left side	ICy Left side	RCx	RCy	FVSA length	Camber gain
0.90°	8.97°	1141.4	-18.0	232.5	-94.3	1554	0.0369°/mm

The coordinates in table 10 above are based on the coordinate system in figure 18, therefore the vertical position of the RC is 67.7 mm below the chassis and 58.3 mm above ground for design height.

The initial camber loss for the front track was 0.0888°/mm, by subtracting the camber gain calculated above we get a total camber loss of 0.0519°/mm. By dividing the total camber loss with the initial camber loss we get a camber loss fraction or “degree camber loss per degree roll” of 0.58.

This is a convenient form since chassis roll is usually measured in degrees, not in mm wheel travel relative to chassis.

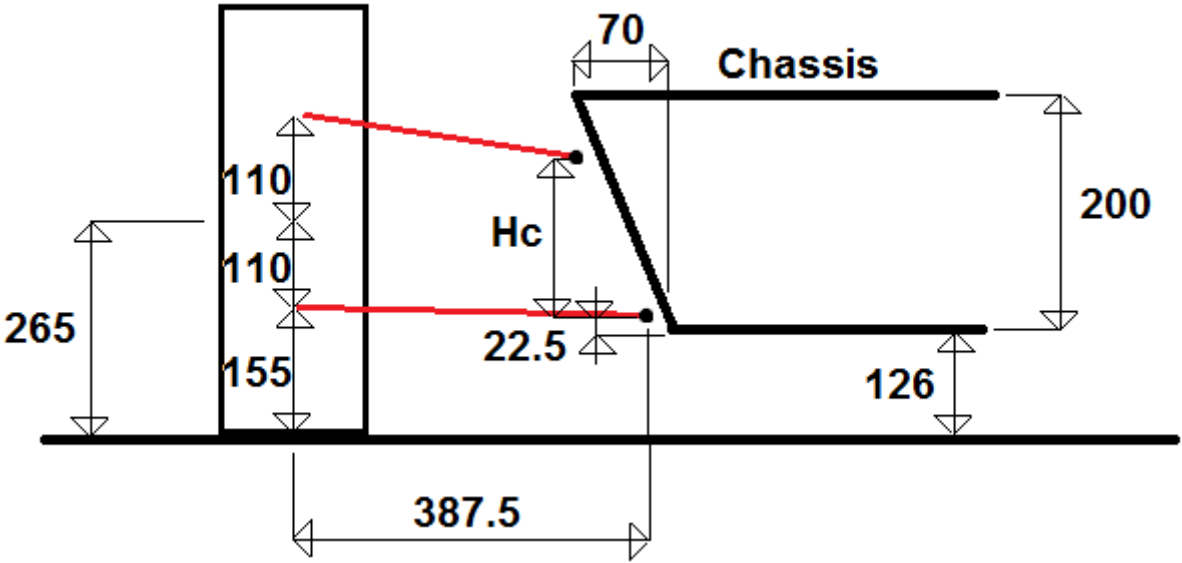


Figure 19. Rear suspension geometry

Table 11. Input for rear suspension geometry

Input								
Δy	L1	L2	L3	L4	L5	L6	L7	L8
6.5	387.5	170	220	317.5	70	155	0	232.5

Table 12. Output for rear suspension geometry

Output							
α	$\beta + \gamma$	ICx Left side	ICy Left side	RCx	RCy	FVSA length	Camber gain
0.96 °	10.25 °	959.0	-16.1	232.5	-87.5	1346.5	0.0426 °/mm

The initial camber loss for the rear track was 0.0924 °/mm. Combined with the camber gain found in table 12 we get a total camber loss of 0.0498 °/mm and a camber loss fraction of 0.54.

Weight Transfer

To determine the necessary stiffness and strength of the suspension the weight transfers which will occur during various handling situations must be found.

Longitudinal weight transfer

Longitudinal weight transfer occurs during longitudinal acceleration, that is, braking and increasing speed. Since the car brakes with all 4 wheels but only accelerates with 2, the acceleration during braking will be larger and thus yield the largest weight transfer. Downforce from aerodynamic devices is larger at high speeds giving the car increased grip for longitudinal acceleration. This does not impact acceleration from the engine to such a degree since the engines reaction force at the tire contact patch is reduced with speed, i.e. the power is limited. The brakes, however, can be considered to have unlimited power to accelerate the car.

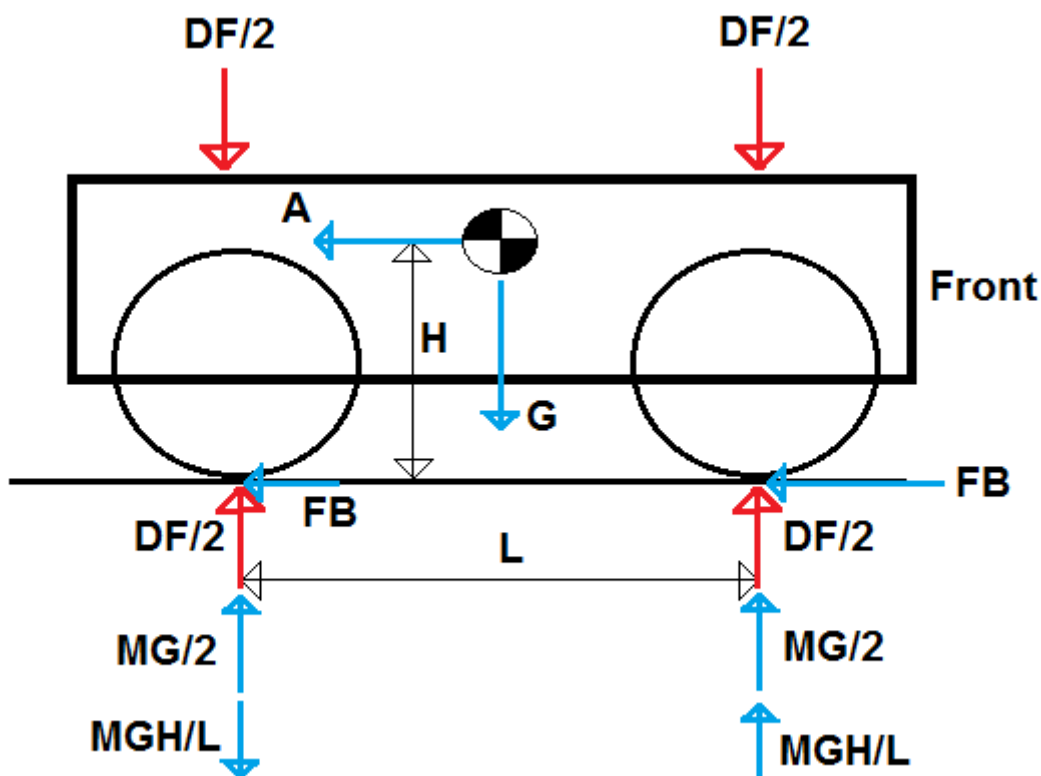


Figure 20. Showing loads on the car during braking

The tracks in Formula Student are designed to limit the top speed to 105 km/h. To have a safety margin the weight transfer calculations will assume a speed of 125 km/h.

The information required to calculate the weight transfer has been summarized in the table below:

Table 13. Input for calculating longitudinal weight transfer

Wheelbase	1600 mm
CoG height	381 mm
Mass	350 kg
Downforce (at 125 km/h)	2700 N
Tire friction coefficient	$1.74 - 1.28 \cdot 10^{-4} \cdot F_N$

To account for tire load sensitivity iterations must be done.

Table 14. Showing load calculations for braking

Iteration	Load per front [N]	Load per rear [N]	Friction front	Friction rear	Brake F per front [N]	Brake F per rear [N]	Brake acc. [m/s ²]	Weight transfer [N]
1	1533	1533	1.544	1.544	2367	2367	27.05	2254
2	2660	406	1.400	1.688	3723	685	25.20	2100
3	2583	483	1.410	1.678	3640	811	25.44	2120
4	2593	473	1.408	1.679	3652	795	25.41	2117
5	2592	474	1.408	1.679	3650	797	25.41	2118
6	2592	474	1.408	1.679	3650	797	25.41	2118

Table 15. Summarizing brake forces for the front

Summary front brake forces per wheel	Per wheel
Maximum brake force	3650 N
Maximum vertical force	2592 N
Load increase from static to 125 km/h due to downforce	676 N
Load increase from weight transfer	1059 N
Total load increase from static to full brake at 125 km/h	1735 N

A diffuser runs along the underside of the chassis leaving a designed ground clearance of 46 mm at the position of the front suspension. The suspension must be stiff enough to avoid ground contact when the total load increase from static till full brake is applied.

	$K_e = 1735 \text{ N}/46 \text{ mm}$	
Effective stiffness, K_e , must be minimum:	$K_e = 37.72 \text{ N}/\text{mm}$	

Since effective stiffness is dependent upon both tire and suspension stiffness an estimate for the tire stiffness is required before minimum suspension stiffness can be determined.

Table 16. Tire stiffness

PSI	Tire load	Static spring rate	N/mm
		lb/in	
17	250	1029	180,2
	350	1101	192,8
	450	1148	201,0
18	250	1059	185,5
	350	1124	196,8
	450	1180	206,6
19	250	1114	195,1
	350	1157	202,6
	450	1216	213,0

Assuming an intermediate pressure of 18 PSI we have a tire stiffness, K_t , of 206.6 N/mm. We define the effective spring stiffness as K_{es} and get the expression:

	$K_e = \frac{K_t * K_{es}}{K_t + K_{es}}$	
By rearranging we get:	$K_{es} = \frac{K_t}{\frac{K_t}{K_e} - 1}$	
Inserting the values:	$K_{es} = 46.14 \text{ N/mm}$	

Transverse stiffness

As previously mentioned transverse stiffness (or roll stiffness) is much more complicated than longitudinal stiffness since the car usually is not symmetric front and rear which it is about the centerline (at least in the design). The use of ARBs and a roll center which is not on the ground further complicates the matter. We start with the easy part, finding the total weight transfer and maximum lateral acceleration.

Table 17. Input for lateral weight transfer

Mean track width	1265 mm
CoG height	381 mm
Mass	350 kg (assumed 50/50 front/rear)
Downforce (at 125 km/h)	2700 N
Tire friction coefficient	$1.74 - 1.28 \cdot 10^{-4} \cdot F_N$

Similar iterations as for braking is needed.

Table 18. Calculations for lateral weight transfer

Iteration	Load per outer [N]	Load per inner [N]	Friction outer	Friction inner	Lat. F per outer [N]	Lat. F per inner [N]	Lateral acc. [m/s ²]	Weight transfer [N]
1	1533	1533	1.544	1.544	2367	2367	27.05	2852
2	2959	107	1.361	1.726	4028	186	24.08	2538
3	2802	264	1.381	1.706	3871	451	24.69	2603
4	2835	232	1.377	1.710	3904	396	24.57	2590
5	2828	238	1.378	1.710	3897	407	24.60	2593
6	2830	237	1.378	1.710	3899	405	24.60	2592

The numbers in table 18 above are inaccurate. They assume that the front and rear track are equally loaded since the mean track has been used. In most cases the front and rear track will not be equally loaded when cornering and thus tire load sensitivity will cause deviation from the total weight transfer and maximum lateral acceleration shown in the table.

To determine the transverse stiffness and the weight transfer for each track the unsprung weight transfer and the weight transfer through the roll centers must be found. The lateral acceleration from the final iteration will be used, $A_L = 24.6 \text{ m/s}^2$

Table 19. Input for lateral weight transfer

Height RC front (all heights relative to ground)	58.3 mm
Height RC rear	61.0 mm
Unsprung weight front	23.0 kg
Height CoG unsprung front	260 mm
Unsprung weight rear	24.6 kg
Height CoG unsprung rear	260 mm
Sprung weight front	152.0 kg
Height CoG sprung front	400 mm
Sprung weight rear	150.4 kg
Height CoG sprung rear	400 mm
Front track width, Tf	1290 mm
Rear track width, Tr	1240 mm

Unsprung weight transfer front:	$\frac{23 \text{ kg} * 260 \text{ mm} * 24.6 \text{ m/s}^2}{1290 \text{ mm}} = 114.0 \text{ N}$	
Unsprung weight transfer rear:	$\frac{24.6 \text{ kg} * 260 \text{ mm} * 24.6 \text{ m/s}^2}{1240 \text{ mm}} = 126.9 \text{ N}$	
Front weight transfer through RC	$\frac{152.0 \text{ kg} * 58.3 \text{ mm} * 24.6 \text{ m/s}^2}{1290 \text{ mm}} = 169.0 \text{ N}$	
Rear weight transfer through RC	$\frac{150.4 \text{ kg} * 61 \text{ mm} * 24.6 \text{ m/s}^2}{1240 \text{ mm}} = 182.0 \text{ N}$	
Mean RC	$\frac{152.0 \text{ kg} * 58.3 \text{ mm} + 150.4 \text{ kg} * 61 \text{ mm}}{302.4 \text{ kg}} = 59.64 \text{ mm}$	
Mean roll moment	$400 \text{ mm} - 59.64 \text{ mm} = 340.36 \text{ mm}$	
Total sprung weight transfer	$\frac{302.4 \text{ kg} * 340.36 \text{ mm} * 24.6 \text{ m/s}^2}{1265 \text{ mm}} = 2001.5 \text{ N}$	

The weight transfer calculated above is independent of the front and rear stiffness. Notice that total sprung weight transfer was not calculated for the front and rear individually but for all of the sprung weight. The total sprung weight transfer is distributed on the front and rear track depending on their relative stiffness.

The suspension stiffness is dependent on the spring stiffness, the motion ration between wheel travel and spring travel, ARB torsional stiffness, motion ratio between spring travel and ARB pick-up point and ARB lever arm. These factors are found through an iterative process of suspension stiffness and component design. To avoid moving back and forth in the thesis the design of components is shown later while factors based on the components will be used here.

To determine the distribution of the sprung weight transfer the following additional information is needed:

Table 20. Input for lateral weight transfer

	Front	Rear
Spring rate, Ks (equivalent of 350 lbs/inch)	61.3 N/mm	61.3 N/mm
MR (Motion Ratio) $\frac{\text{damper travel}}{\text{wheel travel}}$	1.07	1.11
ARB torsional stiffness, Kb	732.8 Nm/rad	773.1 Nm/rad
ARB lever arm length, A (this value is adjustable)	80 mm	110 mm
MR,2 $\frac{\text{ARB rod travel}}{\text{damper travel}}$	0.59	0.41

Table 21. Calculations for lateral weight transfer

	Front	Rear
Bump stiffness	$K_s * MR^2 = 70.2 \text{ N/mm}$	75.5 N/mm
$MR, 3 \frac{\text{ARB rod}}{\text{wheel travel}}$	$\frac{MR, 2}{MR} = 0.55$	0.37
Roll stiffness, without ARB, Tf is front track width	$\frac{K_s * MR^2 * Tf^2}{2} * \frac{\pi}{180^\circ} = 1019 \text{ Nm/}^\circ$	1013 Nm/°
Linear stiffness ARB, Ka	$\frac{K_b}{A^2} = 114.5 \text{ N/mm}$	63.9 N/mm
ARB roll stiffness	$K_a * MR, 3^2 * Tf^2 * \frac{\pi}{180^\circ} = 1014 \text{ Nm/}^\circ$	233 Nm/°
roll stiffness for ARB + springs	2033 Nm/°	1246 Nm°
Total roll stiffness	3279 Nm/°	
Fraction of total	0.62	0.38
Sprung weight transfer	<i>Total sprung transfer * fraction front = 1241 N</i>	761 N
Total weight transfer	<i>Front sprung + front unsprung + front RC = 1524 N</i>	1069 N
Total load on outer	3057 N	2603 N
Total load on inner	10 N	464 N
Total weight transfer	2593 N	
Weight transfer to	<i>Total transfer front – total transfer * fraction front weight = 227 N</i>	–227 N
Resulting roll from lateral acceleration	$\frac{\text{Total sprung transfer * mean roll moment}}{\text{Total roll stiffness}} = 0.77^\circ$	
Roll flexibility, degrees of roll per G of lateral acceleration	$\frac{\text{Resulting roll}}{\frac{\text{Lateral acc.}}{\text{gravity}}} = 0.308 \text{ }^\circ/\text{G}$	
Bump stiffness with ARB	95.6 N/mm	84.9 N/mm
Bump travel transfer fraction	0.36	0.12

The two last rows show the negative effects of the ARB, an increase in bump stiffness and transfer of motion from one wheel to the other when for example a bump is hit. These effects do not occur with synchronous wheel motion such as dive and squat.

Steering axis geometry

A line can be drawn from the upper to the lower wishbone joint towards the wheel. This line is the axis which the upright assembly and wheel revolve around. The angle between this axis and a vertical line is called the caster angle when viewed from the side. When viewed from the front it is called the steering axis inclination (SAI, also known as kingpin inclination, KPI). Caster and SAI cause the camber to change when the wheel is turned.

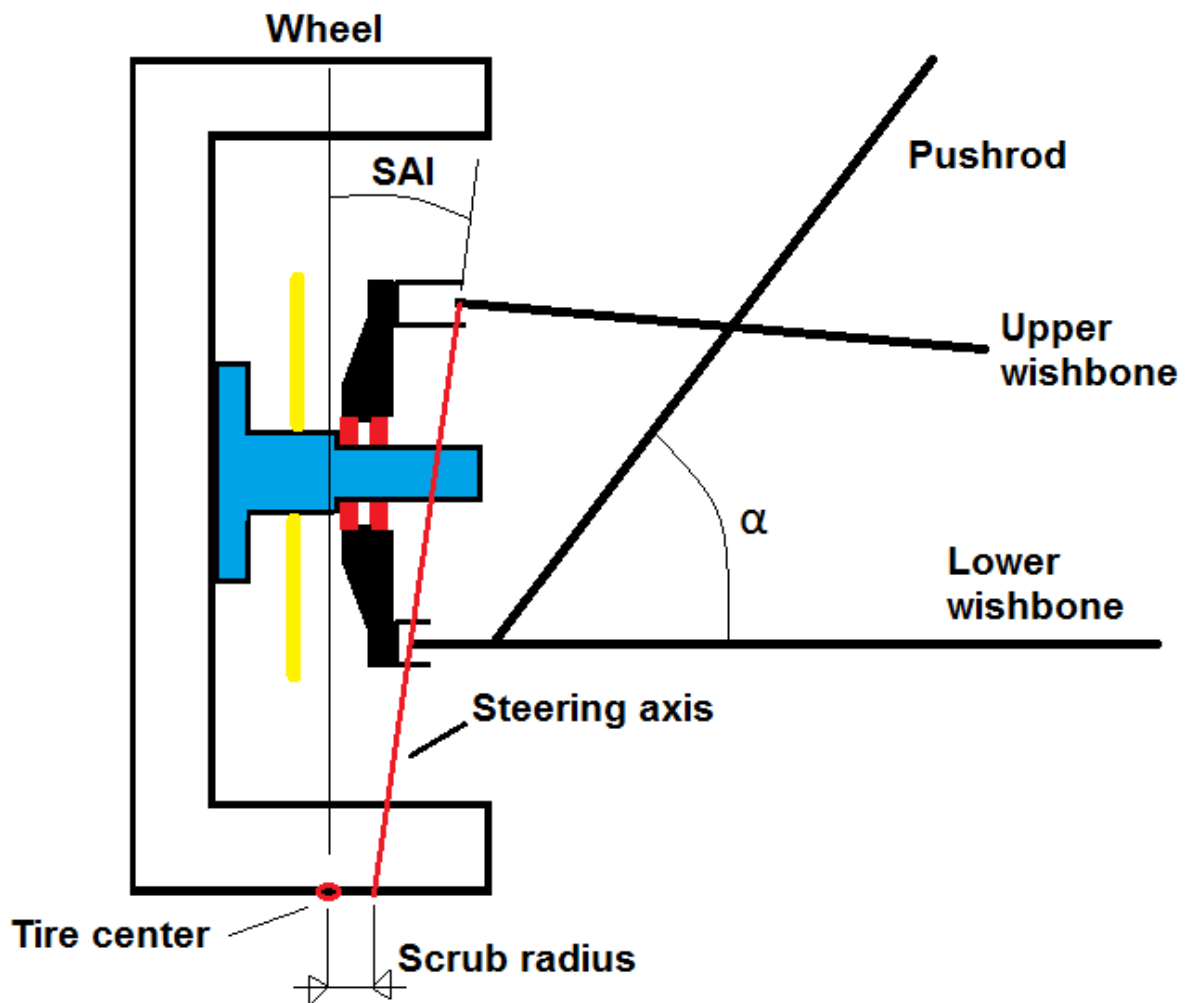


Figure 21. Steering axis geometry in front view

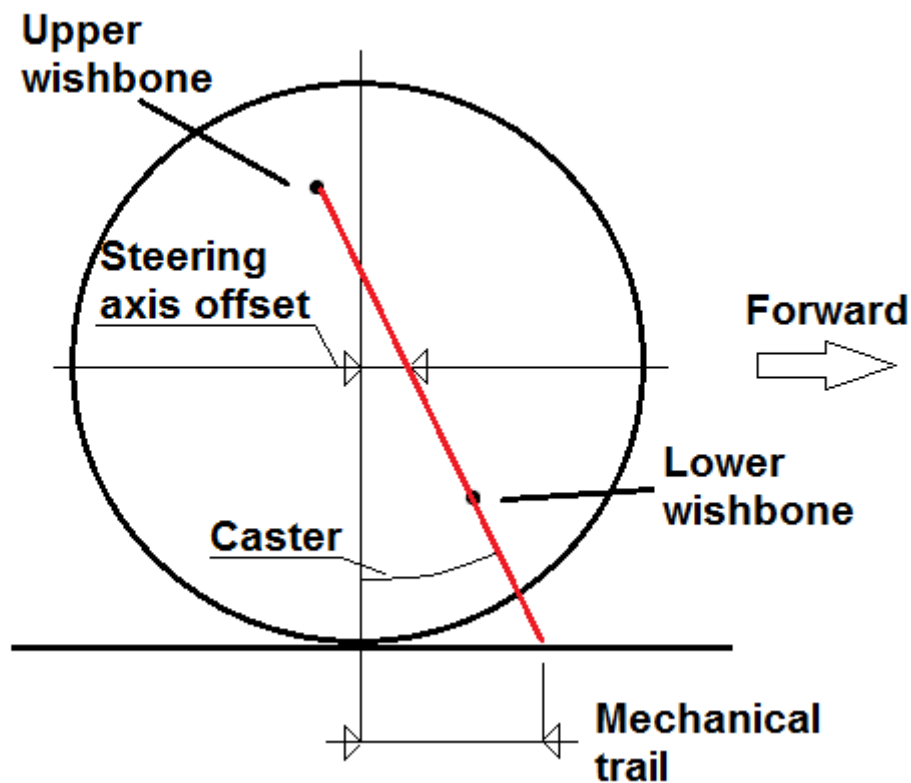


Figure 22. Steering axis geometry in side view

Wheel self-centering is when a wheel returns to its neutral position by forward motion of the car without the driver having to turn it into place. This self-center effect is useful since it keeps the car stable when driving and requires less effort from the driver to realign the wheels after cornering. Self-centering is usually achieved by having mechanical trail. Mechanical trail can be achieved by a caster angle, steering axis offset or both. In addition to self-centering the mechanical trail also increases the steering effort and the loads on the suspension during cornering. Caster has the additional effect of giving negative camber to the outer wheel and positive camber to the inner wheel when cornering which improves the grip.

Scrub (scrub radius) increases the steering effort and the forces in the suspension during braking. Nevertheless some positive scrub can be good since it provides feedback to the driver through the steering wheel during braking.

SAI lifts the car when steering and thus also provides a self-centering effect since the straightforward position will be the lowest position for the car and therefore the equilibrium position. SAI gives positive camber gain on both sides of the car which reduces grip and is the main reason why SAI must be kept small.

The reason for designing suspensions with SAI, other than space requirements, is to reduce the steering effort by reducing the scrub.

The suspension design in this thesis has a scrub of 73.3 mm with 0° SAI while last year's car had a scrub of 62.8 mm. The increase is due to the orientation of the upright with the sloped side towards the wheel. This pushes the brackets on the upright further away from the wheel which increases the scrub. To reduce the scrub the upper wishbone will be slightly shortened while extending the upright bracket for the same wishbone. The wishbone is shortened sufficiently to place the upper upright-wishbone pivot point 9 mm closer to the chassis.

SAI	$\arctan(9mm/220mm) = 2.34^\circ$	
Distance from lower upright-wishbone pivot to ground	$260\text{ mm} - 110\text{ mm} = 150\text{ mm}$	
Resulting scrub	$73.3\text{ m} - 150\text{ mm} * \tan 2.34 = 67.2\text{ mm}$	

Camber loss due to body roll is dependent on lateral acceleration while camber gain due to caster is dependent on the steering angle. Disregarding aerodynamic downforce, a turn with a large radius and a turn with a small radius will produce the same lateral acceleration and thus also the same body roll and camber loss but the tighter turn will require a larger steering angle and thus providing more caster induced camber gain. Aerodynamic downforce increases this effect since it allows better grip at higher speeds increasing the possible lateral acceleration for larger turns.

Regarding the camber changing effects of caster there is no perfect value since a race track will have corners with different radius. To get an idea of how large caster is required the camber loss in a 15 m radius turn will be found. This can be seen as a roughly average turn since turns in the Formula Student competition vary from 4.5 m till 27 m in radius.

Using the excel sheet created for the virtual racetrack it is found that a 15 m turn can result in a lateral acceleration of 17.27 m/s² or 1.76 G. The roll stiffness is 0.308°/G resulting in a body roll of 0.54°, multiplying this with the front camber loss fraction we get a camber loss of 0.314°.

The following equation calculates the steering induced camber gain:

	$Cm = \arccos(\sin(K) \cos(S) + K + \arccos(\sin(Cs) \sin(S)) - 180^\circ$	
--	----------------------------------------------------------------------------	--

Where Cm is camber change, K is SAI (steering axis inclination), Cs is caster and S is steering angle. All input and output is in degrees. The equation is from "Tires, Suspension and Handling" by John C. Dixon.

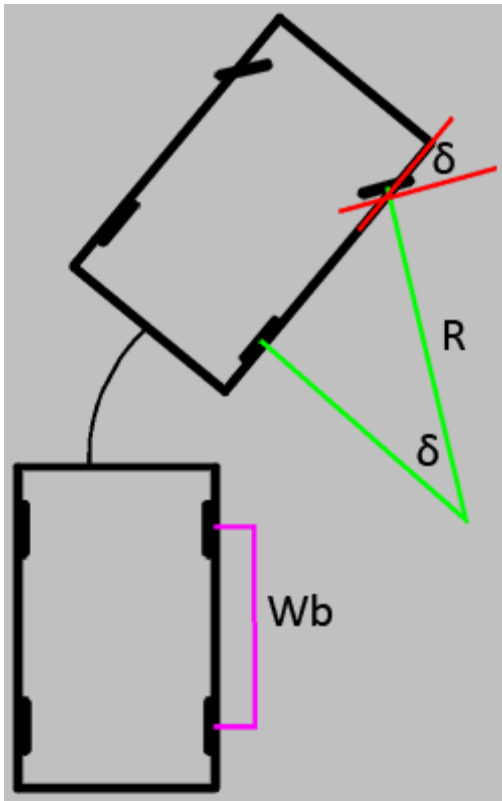


Figure 23. Illustrating steering angle and turning radius. From www.gusongames.com/content/steering.html

In the figure above	$\sin\delta = Wb/R$	
Solving for steering angle	$\delta = \arcsin(Wb/R)$	

Table 22. Camber change vs steering angle

Turn radius, R	Steering angle, δ	Camber change on outer wheel			
		3° caster	4° caster	5° caster	6° caster
5	18.7°	-0.84°	-1.16°	-1.47°	-1.79°
10	9.2°	-0.45°	-0.61°	-0.77°	-0.93°
15	6.1°	-0.31°	-0.41°	-0.52°	-0.63°
20	4.6°	-0.23°	-0.31°	-0.39°	-0.47°
25	3.7°	-0.19°	-0.25°	-0.31°	-0.38°

SAI is 2.34° for all caster angles

The chassis roll for a turn with radius 15 m caused a camber change of 0.314° relative to the ground. For 5° caster the resulting camber is -0.21° on the outer wheel, assuming static camber is set to zero. For tighter turns the resulting absolute camber will be larger while for larger turns the absolute camber will approach zero. The caster will be set to 5° to ensure sufficient camber gain in large turns and good self-centering action. A 5° caster results in: $\tan(5^\circ) * 260 \text{ mm} = 22.7 \text{ mm}$ of mechanical trail.

The distance between the upper and lower pivot point for the upright is 220 mm. $\sin(5^\circ) * 220 \text{ mm} = 19.2 \text{ mm}$. To achieve a 5° caster the lower pivot point will be placed 19.2 mm forward of the upper.

Table 23. Summarizing the designed steering axis geometry

Summary steering axis geometry	
Caster angle	5°
Mechanical trail	22.7 mm
Steering axis offset	0 mm
SAI	2.34°
Scrub radius	67.2 mm

Load Analysis

Before components of the suspension system can be designed the loads resulting from the selected wheel layout, mass distribution and suspension geometry must be determined.

A racing car is truly a dynamic system and to accurately determine the loads for a given handling situation is difficult. To simplify calculations the load analysis will assume static loading situations such as a long constant radius turn and constant deceleration braking. It will be assumed that all the components of the car maintain the same positions relative to one another in these situations.

Since the load analysis will be used to determine the required strength of components the downforce at 125 km/h and a safety factor of 1.3 will be used.

The maximum loads on the suspension have been determined based on the calculations and spreadsheets created for the weight transfer analysis.

Table 24. Design load per wheel, front suspension

Front suspension, load per wheel			
Maximum braking		Maximum cornering	
Vertical load, Fvb	1.3 * 2592 N = 3370 N	Vertical load, Fvc	1.3 * 3296 N = 4285 N
Longitudinal load, Flb	1.3 * 3650 N = 4745 N	Lateral load, Flc	1.3 * 4351 N = 5656 N

The braking and cornering loads given in table 24 above cannot occur simultaneously since the tire friction cannot hold the maximum value in both longitudinal and lateral direction at the same time. Braking and cornering loads can occur simultaneously but the magnitude of each will be significantly reduced. Therefore components of the suspension will be designed for the load case of highest severity but not for braking and cornering loads at the same time.

The cornering loads have been based on the lever arms for the ARBs at 50 mm and 110 mm front and rear respectively resulting 73.9 % of the sprung weight transfer occurring at the front track.

Upright design

The wheel is bolted to the hub which is connected to the upright with two tapered bearings back to back. The bearings are interference fitted onto the hub on the inside and interference fitted into the upright on the outside. A nut with a lock pin presses the assembly together.

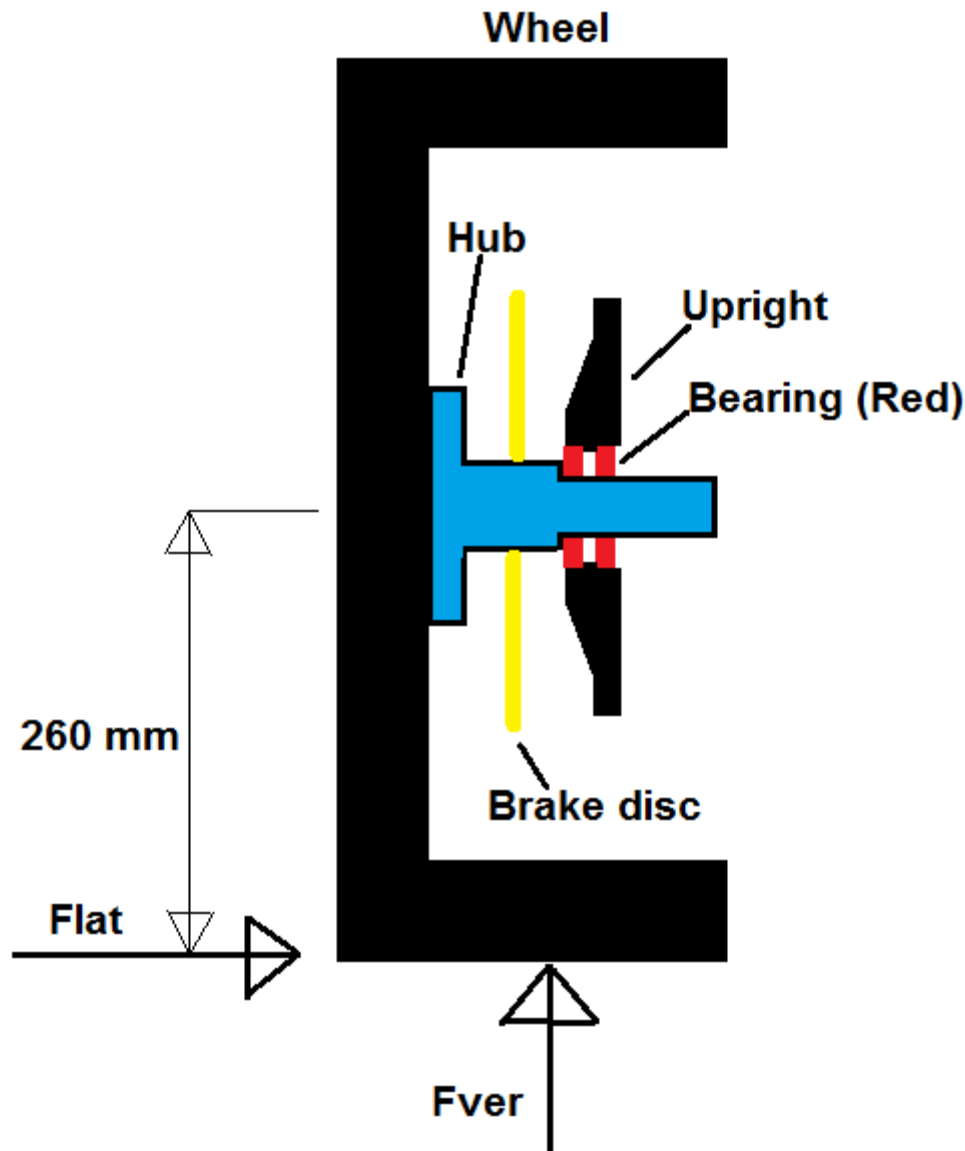


Figure 24. Wheel assembly with loads

The tapered bearings have an inner and outer diameter of 31.75 mm and 58.738 mm respectively and a width of 14.684 mm. To fix the bearings to the upright the upright will be made with integrated bearing housings on both sides. The center of the upright must therefore have holes with a certain depth and a diameter of roughly 58.7 mm. This ensures that the width in longitudinal direction is quite large resulting in a large section modulus about the lateral axis. Since the strength about the lateral axis is inherently high the upright will be designed based on the required bending moment capacity about the longitudinal axis.

The bending moment about the longitudinal axis is the lateral force, Flat, multiplied with the vertical distance from the tire contact patch to the center of the hub. To ensure that the entire capacity of

the upright is not taken by the bending moment the bending moment capacity will be reduced with a factor of 0.8. Since the loads will constantly alter elastic moment capacity will be used as opposed to elastic-plastic to avoid fatigue.

Elastic bending moment capacity:	$\frac{bh^2 * \sigma}{6 * \gamma}$	
	$M = 5656 N * 260 mm \leq \frac{0.8 * bh^2 * \sigma}{6 * \gamma}$	

Where b and h are width (longitudinal) and thickness (laterally) respectively, γ is a material factor and will be set to 1.05, σ is yield stress. The upright will be made in 6082 T6 aluminum giving a yield stress of 288 MPa. To allow sufficient space on the hub h is set to 30 mm.

Solving for b:	$b \geq \frac{5656 N * 260 mm * 6 * \gamma}{0.8 * (30 mm)^2 * 288 MPa} = 44.7 mm$	

The bending moment will be reduced when moving from the upright center towards the brackets for the wishbones. Therefore the upright will be progressively thinner when moving away from the center. At the top and bottom of the upright the brackets holding the wishbones will be fastened with bolts and lock nuts. To have sufficient space for the lock nuts between the upright and the brake disc the sloped side has been placed towards the wheel.

The bearings are made with an outside diameter of 58.738 mm $\frac{+25 \mu m}{-0 \mu m}$ and the upright will be machined with a precision of $\pm 5 \mu m$. To ensure an interference fit of minimum 5 μm the upright diameter is set to 58.728 mm giving a maximum and minimum interference of 40 μm and 5 μm respectively.

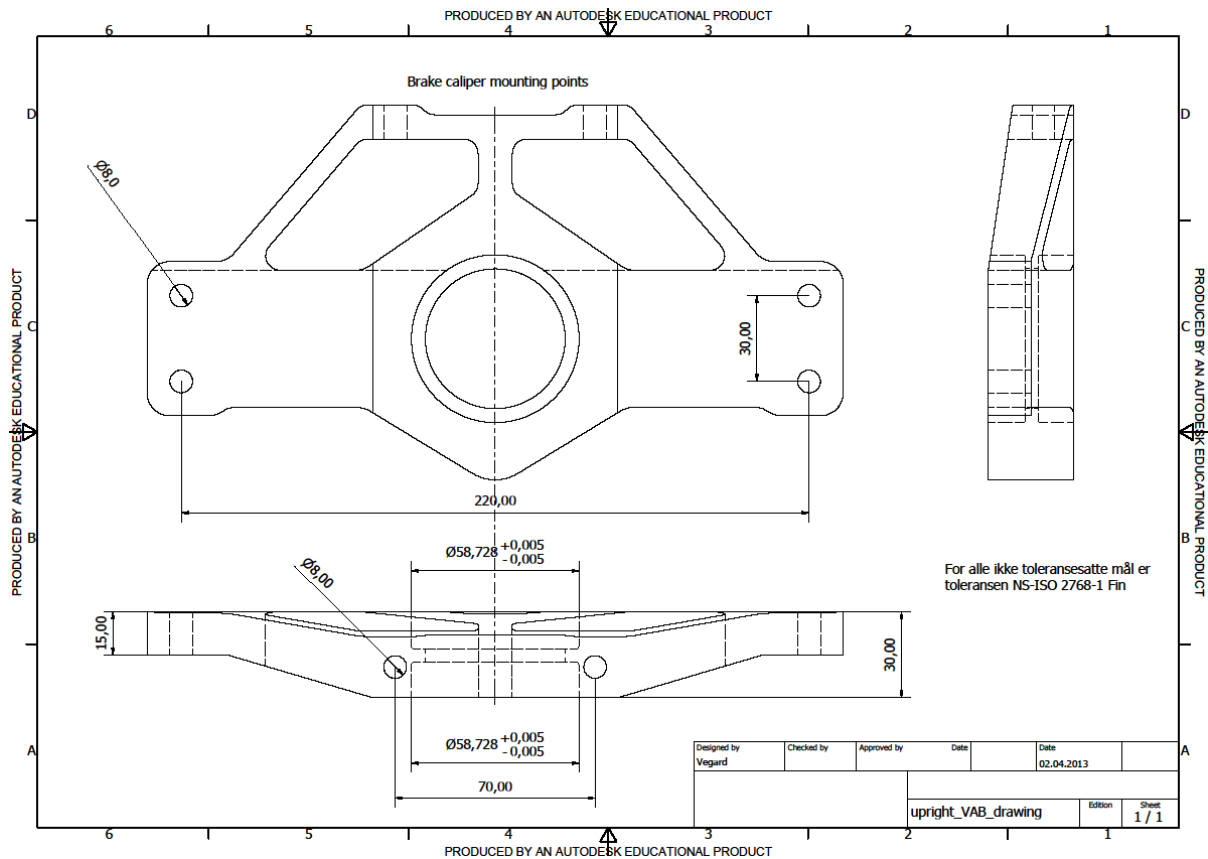


Figure 25. Front upright

Since the upright is a complicated and critical part an additional finite element analysis (FEA) was conducted. The loading situation between the bearings and the upright cannot be accurately simulated in Autodesk Inventor using the integrated restraint function. This is because the bearings will only transfer compressive forces to the upright since it has not been fastened with welds or bolts. To overcome this obstacle a dummy hub with bearings was mounted into the upright with an interference fit. The dummy hub was restrained from all rotation and motion and the reaction forces from the upright brackets were applied.

The lower reaction force is:	$\frac{5656 N * 260 mm}{260 mm + 110 mm} = 9513 N$	Acting towards wheel
The upper reaction force is:	$9513 N - 5656 N = 3857 N$	Acting towards chassis

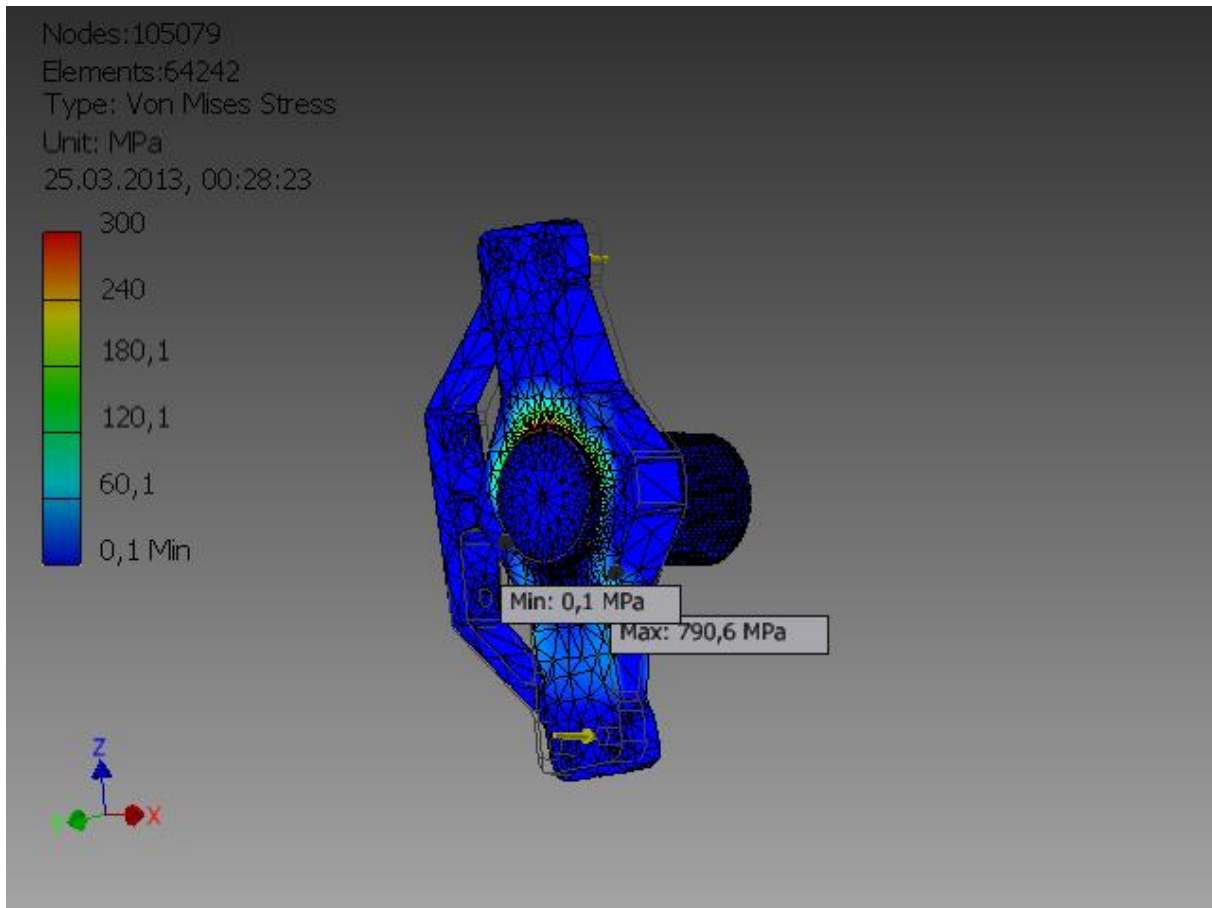


Figure 26. FEA of front upright. Analysis done in Autodesk Inventor

The rated maximum stress can be disregarded since it occurs in the dummy hub. Stresses in the contact areas reached 300 MPa which is high but will be lower in reality since local yielding will give a more evenly distributed loading. In the design code for steel structures, Eurocode 3, local yielding in connection points are allowed thus the FEA controlled upright design is approved and will be issued for manufacturing. Notice how the upright is practically unstressed in the area below the bearing in figure 26, if the upright was fastened to the hub with welds instead of an interference fit this area would experience tensile stresses.

Pushrod design

The pushrod will be bolted to brackets on the lower wishbone on one side and to the rocker on the other side. To minimize bending moment on the lower wishbone the brackets for the pushrod will be placed as close to the wheel as possible. For design calculations, however, a conservative 50 mm transverse distance between the connection points for the pushrod and the upright on the wishbone will be assumed.

The pushrods are made by welding a steel insert into each end of a steel tube. The inserts have threaded holes which a rod end can be placed in. To secure the position of the rod end in the insert a counter nut is tightened against the insert. By using left and right handed threads at the bottom and top of the pushrod respectively the total length of the pushrod can be altered without removing

either of the rod ends. The adjustability is no more than roughly 20 mm but it is sufficient to adjust the cross weight of the car.

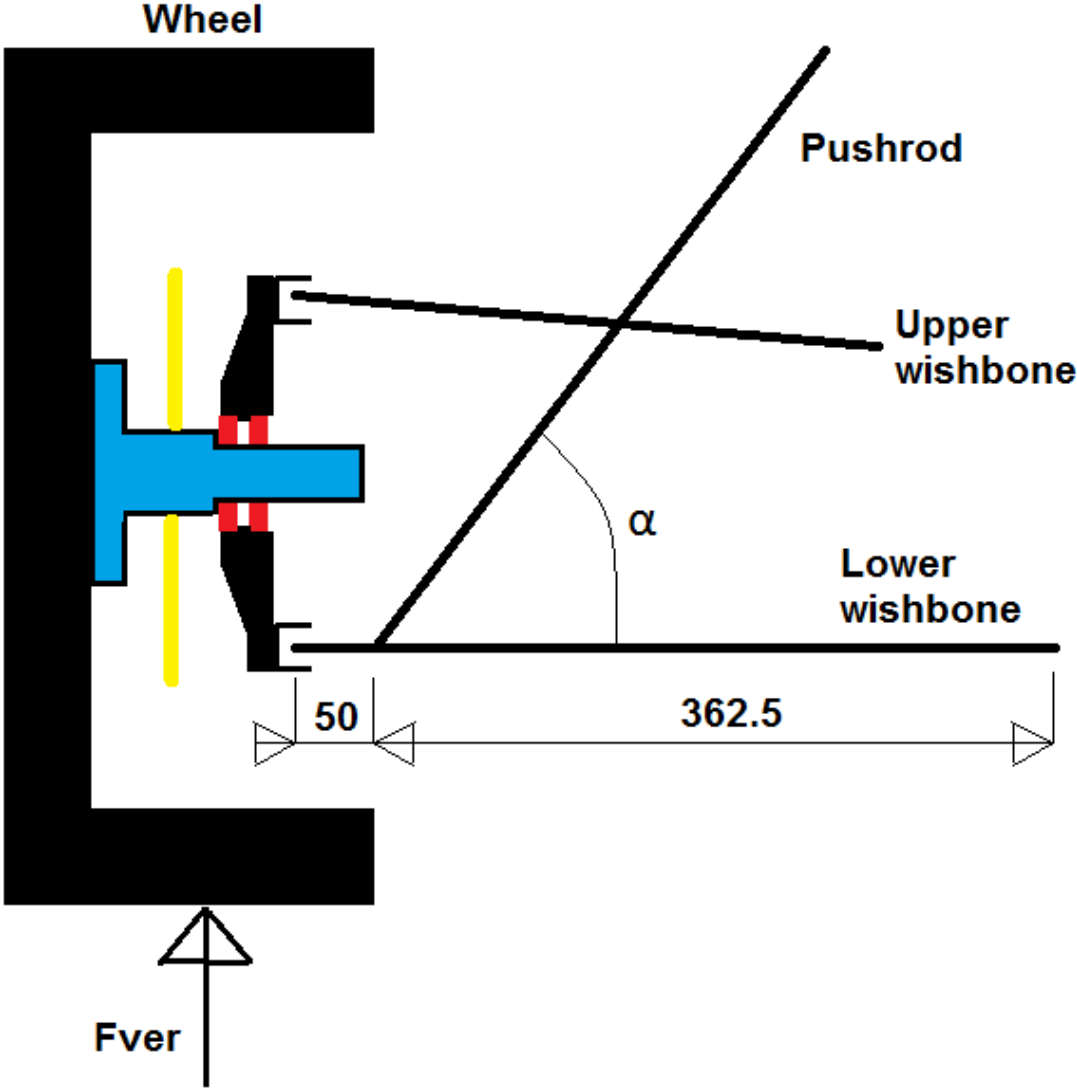


Figure 27. Wheel assembly with wishbones and pushrod

The angle α is the effective 3 dimensional angle between the pushrod and the horizontal plane, not the front view or side view angle. α is 62 ° for the front pushrod.

Pushrod vertical component:	$\frac{4285 N * (50 + 362.5) mm}{362.5 mm} = 4876 N$	
Actual pushrod load:	$\frac{4876 N}{\sin(62^\circ)} = 5522 N$	

The pushrod tube has an outer diameter of 19.05 mm, a wall thickness of 0.889 mm, a total length of 520 mm and is made from 4130 steel with a yield stress of 650 MPa. Buckling capacity calculations according to Eurocode 3 are shown below.

Table 25. Input and calculations for pushrod

Outer diameter, Do	19.05 mm	
Inner diameter, Di	17.272 mm	
Yield stress, σ	650 MPa	
Critical length, Lcr	520 mm	Critical length same as length for column pinned at both ends
Material factor, γ	1.05	
α	0.49	Eurocode 3, imperfection factor, cold formed circular tube
Cross sectional area, A	$\frac{\pi(D_o^2 - D_i^2)}{4} = 50.72 \text{ mm}^2$	
Second moment of inertia, I	$\frac{\pi(D_o^4 - D_i^4)}{64} = 2096 \text{ mm}^4$	
Radius of gyration, i	$\sqrt{I/A} = 6.43 \text{ mm}$	
Material strength correction factor, ϵ	$\sqrt{235 \text{ MPa}/\sigma} = 0.601$	
Class check	$70\epsilon^2 > \frac{D_o}{t}$ $25.3 > 21.4$	t is wall thickness Cross section is class 2
Slenderness value, λ_1	$93.9\epsilon = 56.5$	
Non-dimensional slenderness, λ	$\frac{L_{cr}}{i * \lambda_1} = 1.433$	
ϕ	$0.5[1 + \alpha(\lambda - 0.2) - \lambda^2] = 1.828$	
Buckling reduction factor, χ	$\frac{1}{\phi + (\phi^2 - \lambda^2)^2} = 0.337$	
Buckling capacity, Nb	$\frac{\chi * A * \sigma}{\gamma} = 10593 \text{ N} > 5522 \text{ N}$	Tube capacity is larger than load
M8 Rod end capacity, SA 8 C (provided by manufacturer)	12900 N > 5522 N	Rod end capacity is larger than load
Weld between tube and insert	OK by inspection	Buckling utilization of tube is low, weld has same area as tube and the weld is not susceptible to buckling

The pushrod is connected to wishbone and rocker using M8 bolts with grade 12.9. The bolts go through the brackets with the pushrod rod end in the middle. To allow angular motion of the pushrod the span between the brackets are 16 mm while the rod end is only 8 mm thick. This causes the bolt to be loaded in bending.

Table 26. Calculations for bolt securing the pushrod

M8, 12.9 bending capacity, unthreaded section	$\frac{1080 \text{ MPa} * \pi * (8 \text{ mm})^3}{32 * 1.05} = 51702 \text{ Nmm}$	
Applied bending moment, to be conservative full span is used	$\frac{F * L}{4} = \frac{5522 \text{ N} * 16 \text{ mm}}{4} = 22088 \text{ Nmm}$	
	$5702 \text{ Nmm} > 22088 \text{ Nmm}$	Load is less than capacity
Elastic shear capacity	$\frac{0.6 * 1080 \text{ MPa} * \pi * (8 \text{ mm})^2}{4 * 1.05} = 31021 \text{ N}$	
Shear utilization	$\frac{5522 \text{ N}}{31021 \text{ N}} = 0.18$	Since utilization is less than 50 %, no reduction of bending capacity

Table 27. Design loads rear suspension, per wheel

Rear suspension	
Maximum cornering	
Vertical load	$1.3 * 3001 \text{ N} = 3901 \text{ N}$
Lateral load	$1.3 * 4049 \text{ N} = 5264 \text{ N}$

The cornering loads for the rear suspension have been based on the lever arms for the ARBs at 110 mm and 50 mm front and rear respectively resulting in 57.9 % of the sprung weight transfer occurring at the rear track. Braking and acceleration loads are small compared to the cornering loads for the rear suspension and has been omitted.

The strength calculations for the rear suspension components are similar as those for the front and therefore they will not be shown in this thesis.

Rocker design

To transfer the load from the pushrod to the springs and ARB a rocker (also known as bell crank lever) is used. The rocker can be designed to give the desired motion ratio (MR) between wheel travel, spring/damper movement and ARB movement.

The FSAE rules require a total wheel travel of 50.8 mm (2 inches) and the Ohlins TTX25 have a stroke length of 57 mm which limit the MR for $\frac{\text{wheel travel}}{\text{spring motion}}$ to 1.12. The angle between the pushrod and the horizontal plane and the pushrod attachment point on the lower wishbone also affect the MR and must be found before the rockers can be designed.

For strength calculations the distance between the pushrod attachment point and upright-wishbone connection point was conservatively set to 50 mm. Here we will assume it is zero since that is what

we want to achieve in the wishbone design. The angle between the pushrod and the horizontal plane was (α in figure 21) is 62° for the front and 54° for the rear.

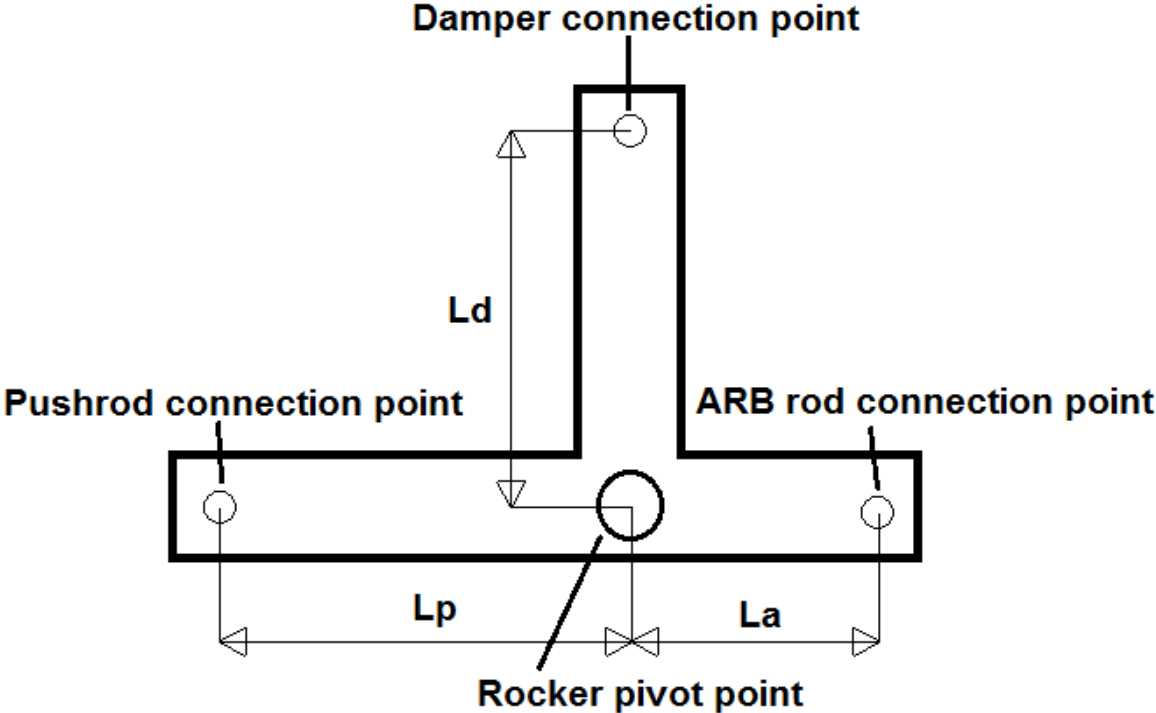


Figure 28. Illustration of rocker

For both the front and the rear rocker the distance between the damper connection point and the rocker pivot point, L_d , will be set to 110 mm. This distance has been chosen since it places the dampers roughly perpendicular to the rocker motion for the damper connection points on the frame.

The angles between the rocker motion and the rods connected to it will change slightly during wheel travel but to simplify calculations they will be assumed to remain perpendicular.

The distance from the pushrod connection point and the rocker pivot point, L_p , will be determined so that the MR approaches 1.12, this gives the maximum stiffness for a given spring rate.

To determine L_p for front rocker	$\frac{110 \text{ mm}}{L_p} * \sin 62^\circ = 1.12$	
	$L_p = 86.7 \text{ mm} \rightarrow \text{use } 90 \text{ mm}$	
Resulting front MR	$\frac{110 \text{ mm}}{90 \text{ mm}} * \sin 62^\circ = 1.07$	
To determine L_p for rear rocker	$\frac{110 \text{ mm}}{L_p} * \sin 54^\circ = 1.12$	
	$L_p = 79.5 \text{ mm} \rightarrow \text{use } 80 \text{ mm}$	
Resulting rear MR	$\frac{110 \text{ mm}}{80 \text{ mm}} * \sin 54^\circ = 1.11$	

L_a is the distance between the rocker pivot point and the connection point for the ARB rod. A large L_a increases the effect of the ARB since it causes larger ARB motion for a given wheel travel. The effect of the ARB can also be increased by increasing the torsional stiffness of the ARB or by

connecting the ARB rod closer to the ARB (i.e. a smaller lever arm) therefore the most desirable effect of a long L_a is the decreased load on the ARB rod and the ARB lever arm. The relationship between L_a and lever arm must be considered to avoid excessive rotation of the lever arm due to wheel travel since this changes the ARB stiffness.

L_a also determines the position of the ARB rod which has been the limiting factor in this design. Front L_a is set to 65 mm to give clearance between the ARB rod and the pushrod and body. For the rear L_a is set to 45 mm to enable the ARB rod to be positioned between the chassis tubes.

A needle bearing is interference fitted into the pivot point of the rockers. A bolt through two brackets on the frame pass through the needle bearing and establishes the pivot axis for the rockers. The rockers are machined in 6082 T6 aluminum.

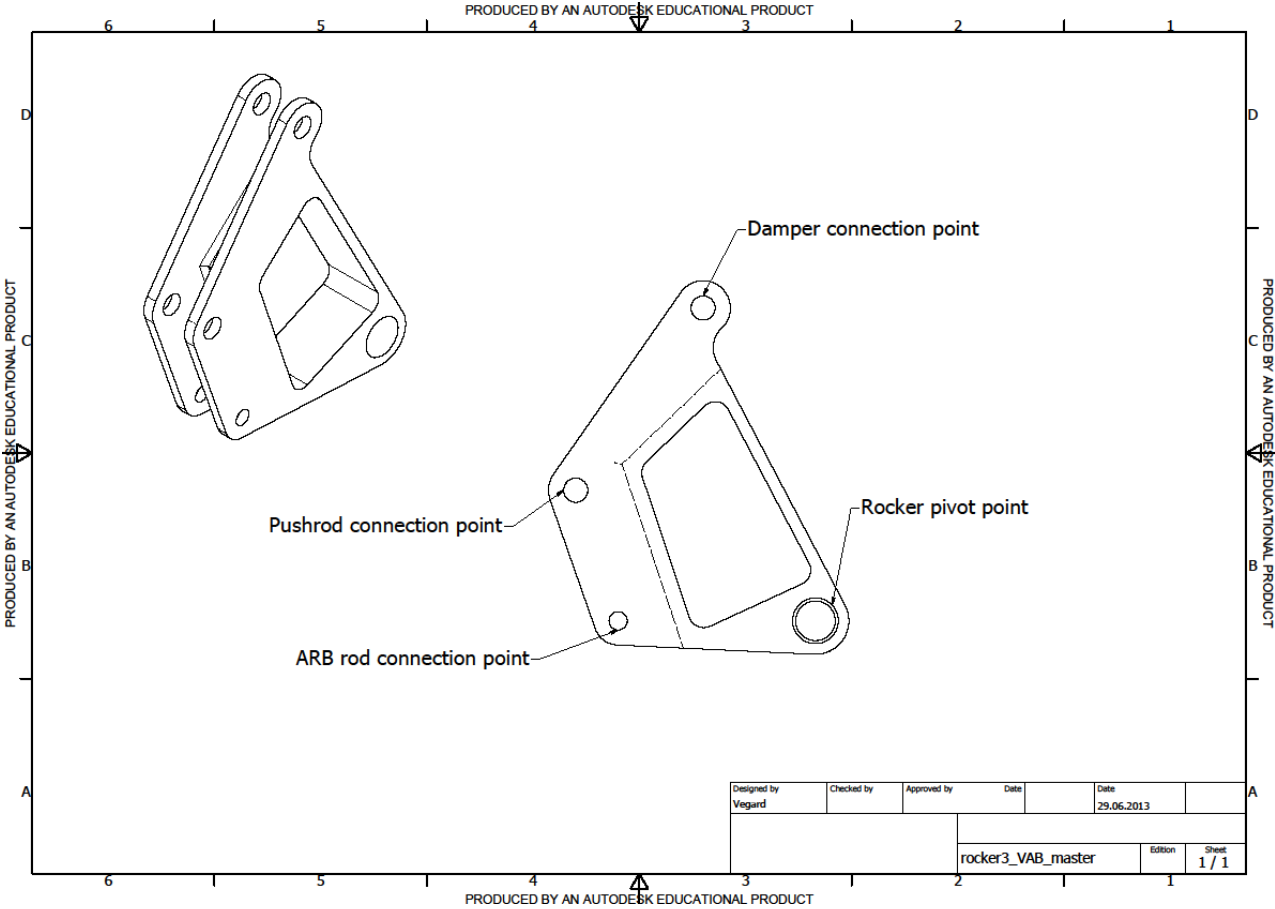


Figure 29. Front rocker

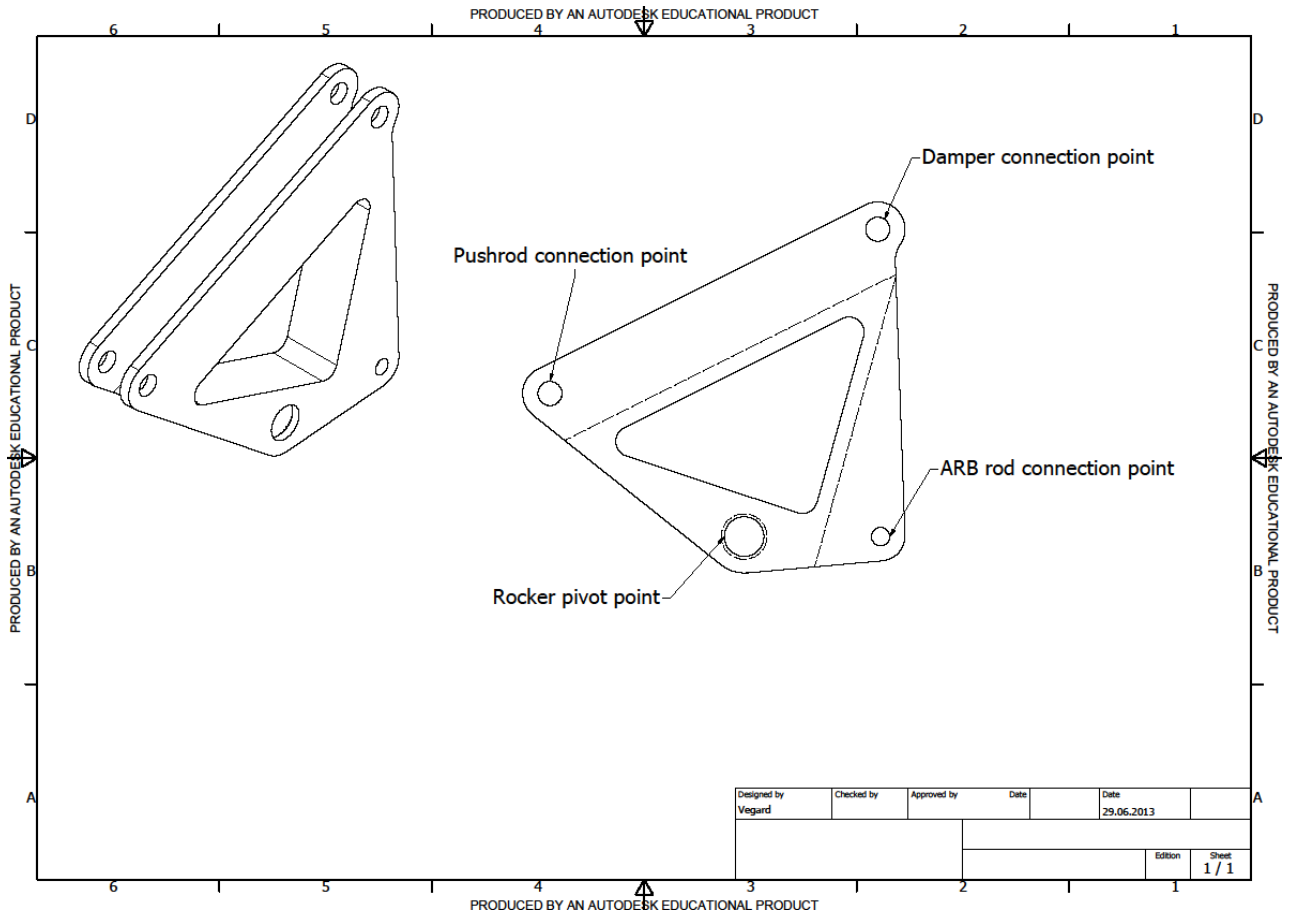


Figure 30. Rear rocker

ARB design

The table below summarizes the required information to calculate the torsional stiffness of the front and rear ARB

Table 28. Input for calculating ARB stiffness

	Front	Rear
Shear modulus steel, G	79.3 GPa	79.3 GPa
Length, L	600 mm	430 mm
Outer diameter, Do	19.05 mm	19.05 mm
Inner diameter, Di	16.56 mm	17.27 mm

For a tube, polar moment of inertia, I_p , is given by:	$\frac{\pi(D_o^4 - D_i^4)}{32} = I_p$	
The equation for torsional stiffness, K_b :	$K_b = \frac{M}{\theta} = \frac{I_p * G}{L}$	

Where M is the applied bending moment, θ is the angular deflection in radians. For I_p in mm^4 , G in MPa and L in mm we get K_b in Nmm/rad .

The torsional stiffness can be found in table 29 below.

To convert to rotational motion of the ARB to a linear motion compatible with the ARB rod a lever arm is connected to each side of the ARB. The length of this lever arm is adjustable but we need an expression relating the torsional stiffness of the ARB and lever arm length to linear stiffness for the ARB rod.

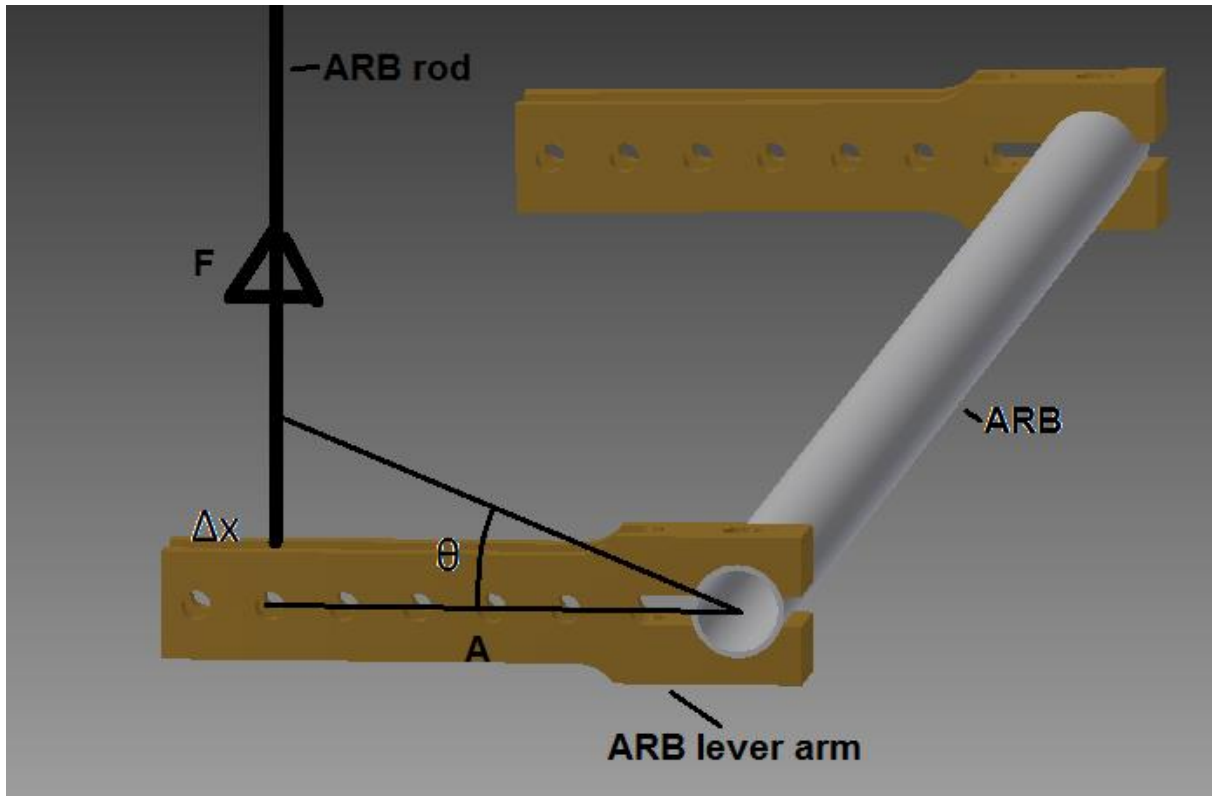


Figure 31. ARB with ARB lever arms

For small angles	$\frac{\Delta x}{A} = \tan\theta \approx \theta$	
	$M = F * A = \frac{I_p * G * \theta}{L} = K_b * \theta$	
Solving for force, F	$F = \frac{K_b * \theta}{A}$	
Inserting for θ	$F = \frac{K_b}{A} * \frac{\Delta x}{A}$	
Linear stiffness for ARB, K_a	$K_a = \frac{F}{\Delta x} = \frac{K_b}{A^2} = \frac{I_p * G}{L * A^2}$	

Table 29. Summary rocker and ARB

	Front	Rear
Lp	90 mm	80 mm
Ld	110 mm	110 mm
La	65 mm	45 mm
Pushrod angle with horizontal plane, α	62°	54°
Motion ratio, damper to wheel travel	1.07	1.11
Motion ratio, ARB lever to damper motion	0.59	0.41
Torsional stiffness ARB	732.8 Nm/rad	773.1 Nm/rad
Possible lengths for ARB lever arm, A	35 mm, 50 mm, 65 mm, 80 mm 95 mm, 110 mm	35 mm, 50 mm, 65 mm, 80 mm 95 mm, 110 mm

Conclusion

Analysis in the virtual racetrack showed that reducing the height to the CoG reduced the lap time. Reducing the height to the CoG reduces the weight transfer during acceleration which reduces the negative effects of tire load sensitivity. This also reduces loads on the suspension and chassis which in turn means that lighter components/chassis can be used and the required stiffness is reduced. These effects were not accounted for but enforce the importance of keeping the CoG as low as possible.

Analysis was also done for different car weights to quantify the performance reduction imposed by added weight. This was found to be roughly 0.062 %/kg of added weight.

Increasing the mean track and the wheelbase both increased the performance, similarly as reducing the CoG height, this has the effect of decreasing the weight transfer. The analysis does not consider the added weight for increasing wheelbase and track width and the effect of maneuvering a larger car through a tight course. These effects should also be considered if drastic changes are considered. Nevertheless the rear track was increased from 1188 mm to 1240 mm to increase the cornering ability of the car.

The analysis revealed an increase in performance with increased rearwards weight distribution as high as 70/30 rear/front. This weight distribution causes the cornering ability to deteriorate but gave sufficient improvement for acceleration and braking to reduce the total lap time. The car was still designed with a 50/50 weight distribution due to all the complicating effects of reduced cornering ability such as over/understeer but this is a recommended area for further analysis.

Bump stiffness was designed based on required ground clearance during maximum acceleration. Since the track width is smaller than the wheelbase the car is inherently softer during lateral acceleration as opposed to longitudinal (e.g. braking) but the use of ARBs effectively increased the lateral stiffness (i.e. roll stiffness) without too much increase in bump stiffness. The use of adjustable ARBs also allows the roll stiffness and the sprung weight transfer distribution to be adjusted.

The suspension geometry was designed to minimize scrub and jacking while having good camber gain and roll center height. The camber gain front and rear is 0.0369 °/mm and 0.0426 °/mm respectively corresponding to a camber loss fraction of 0.58 and 0.54 respectively. The roll center front and rear is 58.3 mm and 61 mm above the ground respectively. This height ensures that jacking and scrub are kept low while there is a large roll moment giving a large amount of sprung weight transfer which can be distributed between the front and rear track depending on chosen ARB stiffness's.

References

CEN, (2005), Eurocode 3: Design of steel structures – Part 1-1: General rules and rules for buildings, CEN, Brussel.

Gustafson, S.Å. (2007), Lecture Notes Course ÅMA 190, Numerical Mathematics, First Course, Stavanger.

Milliken, W.F. and D.L. Milliken (1995), Race Car Vehicle Dynamics, Society of Automotive Engineers, U.S.A.

Rottmann, K. (2006), Matematisk Formelsamling, 9. Opplag, Spektrum Forlag.

Staniforth, A. (2010), Competition Car Suspension, 4th edition, Haynes Publishing, UK.

FSAE 2013 rules

FS 2013 rules

Appendix A – Virtual Racetrack Setup

This appendix describes the setup of the virtual racetrack used in the Suspension Layout chapter.

FSAE rules specify that the endurance and sprint track should be designed such that the top speed is 105 km/h and that the average speed is 48 – 57 km/h. The virtual racetrack will be made as an oval racetrack and the radius of the turns and the length of the straights are adjusted to ensure a fair resemblance to the endurance and sprint track.

The radius of the turns, R , will be such that maximum cornering speed is 40 km/h and the straights will have a length, L , such that a top speed of 105 km/h can be achieved before braking down to 40 km/h before the turn.

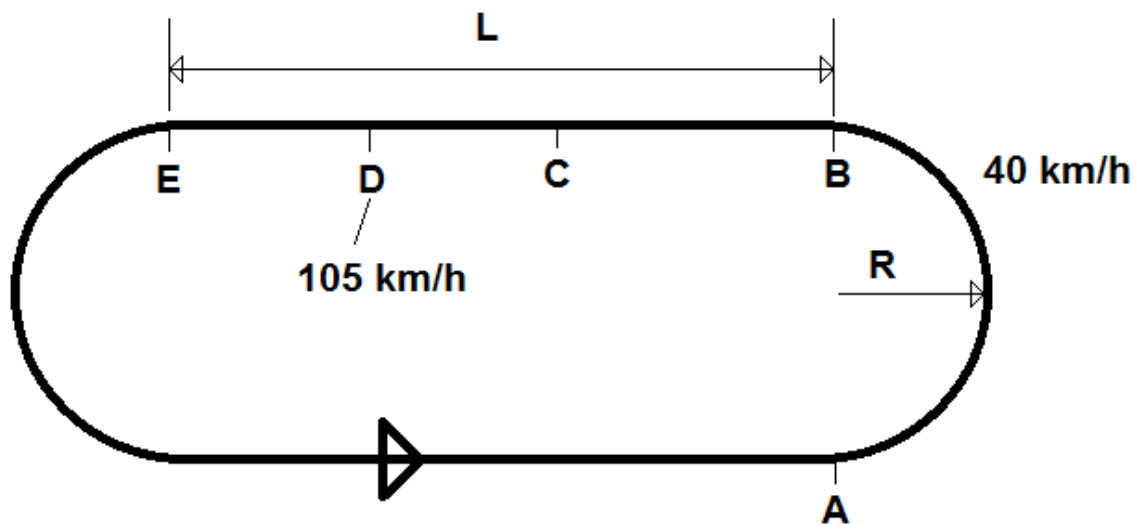


Figure 32. Virtual racetrack with design speeds

The racetrack will be designed based on car with a total weight, m , of 350 kg, an engine power of 59.6 kW constantly and a tire friction of $1.74 - 1.28 \cdot 10^{-4} \cdot F_N$, where F_N is the normal tire force. Weight transfer and aerodynamic downforce and drag will be neglected to simplify the calculations.

F_N	$\frac{350 \text{ kg}}{4} * 9.81 \text{ m/s}^2 = 858.4 \text{ N}$	
Tire friction	$1.74 - 1.28 * 10^{-4} * 858.4 = 1.63$	

Neglecting weight transfer and downforce the tire friction will be 1.63 constantly which gives lateral and braking accelerations of 1.63 G and grip limited acceleration of 0.815 G.

Cornering speed, V_c	$40 \text{ km/h} = 11.11 \text{ m/s}$	
	$\frac{(11.11 \text{ m/s})^2}{R} = 1.63 * 9.81 \text{ m/s}^2$	
Solving for R	$R = 7.7 \text{ m}$	
Cornering time:	$\frac{7.7 \text{ m} * \pi}{11.11 \text{ m/s}} = 2.18 \text{ s}$	

For low speed the grip will be the limiting factor for the acceleration, at higher speeds the engine power will be the limiting factor. The point C indicates the position of this transition.

Grip limited acceleration, A_g :	$0.815 * 9.81 \text{ m/s}^2 = 8.00 \text{ m/s}^2$	
Power equation:	$P = A_g * M * V$	
Top grip limited speed:	$V_p = \frac{P}{A_g * M} = 21.30 \text{ m/s}$	

P is the engine power of 59.6 kW

The top grip-limited speed, V_p , is the speed where the engine power becomes the limiting factor. Up to this speed the car will accelerate with 8 m/s^2 constantly. Since the corner exit speed is known the required time and distance from corner exit till V_p is reached can be found. This is the distance B to C in the figure above.

Time from corner exit till V_p is reached, t_1	$t_1 = \frac{V_p - V_c}{A_g} = 1.27 \text{ s}$	
Constant acceleration gives an average speed of:	$\frac{V_p + V_c}{2} = 16.20 \text{ m/s}$	
Distance from B to C	$16.20 \text{ m/s} * 1.27 \text{ s} = 20.65 \text{ m}$	

After V_p the acceleration is no longer constant and the time required to reach top speed is found by calculating the time to reach the kinetic energy at top speed.

	$Ek = 0.5 * M * V^2 = P * t$	
	$\Delta Ek = 0.5 * M * (Vt^2 - Vp^2) = P * \Delta t$	
Solving for Δt :	$\Delta t = 1.166 \text{ s}$	

Need to find an expression for speed as a function of time in the power-limited region to determine the distance from C to D now that we have the time.

Exchanging V_t with $V(t)$ and solving for $V(t)$	$V(t) = \sqrt{\frac{2 * P * t}{M} + V_p^2}$	
	$x(t) = \int V(t) dt$	

To simplify: $a=2P/M$	$x(t) = \frac{2}{(2+1)a} (at + Vp^2)^{1+0.5} + C$ $x(t) = \frac{2}{3a} (at + Vp^2)^{\frac{3}{2}} + C$	
-----------------------	-------------------------------------------------------------------------------------------------------	--

x and t are both set to zero at point D.

	$x(0) = 0 = \frac{2}{3a} Vp^3 + C$	
	$C = -\frac{2}{3a} Vp^3$	
	$x(t) = \frac{2}{3a} (at + Vp^2)^{\frac{3}{2}} - \frac{2}{3a} Vp^3$	
Power-limited distance, from C to D	$x(1.166) = \frac{2}{3a} (at + Vp^2)^{\frac{3}{2}} - \frac{2}{3a} Vp^3 = 29.66 \text{ m}$	

The braking acceleration, A_b , is the same as the lateral acceleration only in opposite direction.

Time to decelerate from top speed to cornering speed, t_3	$t_3 = \frac{V_c - V_t}{A_b} = 1.13 \text{ s}$	
Average speed when braking	$\frac{V_t + V_c}{2} = 20.14 \text{ m/s}$	
Braking distance, D to E	$20.14 \text{ m/s} * 1.13 \text{ s} = 22.76 \text{ m}$	
Length of straight, B to E	$22.76 \text{ m} + 29.66 \text{ m} + 20.65 \text{ m} = 73.07 \text{ m} \approx 73 \text{ m}$	
Track length	$73 \text{ m} * 2 + 7.7 \text{ m} * \pi * 2 = 194.4 \text{ m}$	
Average speed for calculations	$\frac{194.4 \text{ m}}{1.13 \text{ s} + 1.166 \text{ s} + 1.27 \text{ s} + 2.18 \text{ s}} = 16.97 \text{ m/s}$ $= 61.1 \text{ km/h}$	

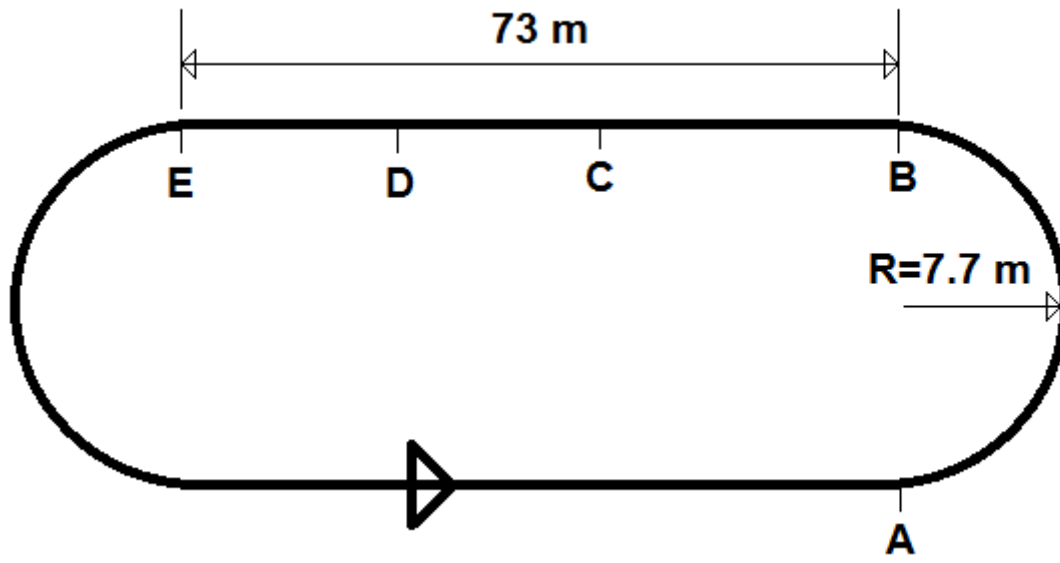


Figure 33. Virtual racetrack with dimensions

Appendix B – Performance Analysis in Virtual Racetrack

In this appendix the calculations used to determine a cars performance in the virtual racetrack for various parameters are shown. To easily change the parameters and get the new output an excel sheet has been used for the actual calculations.

Cornering

Table 30. Input for cornering calculations

Mass	350 kg
Height CoG	381 mm
Mean track width	1265 mm
Fraction of weight on heavy side	0.6
Downforce coefficient	2.239
Turning radius	7.7 m
Tire friction coefficient	$1.74 - 1.28 \cdot 10^{-4} \cdot F_N$

The calculations are very similar to those in Weight Transfer, the difference is:

- The speed and therefor the downforce is initially unknown and must also be calculated for each iteration. Speed is found based on the calculated lateral acceleration and the given turning radius. Downforce is then calculated from the speed and the downforce coefficient.
- The inputs make it possible to have on end of the car heavier than the other. These calculations are based on the heavily loaded end. The heavy end will be capable of the least lateral acceleration because tire load sensitivity and an evenly distributed downforce will give this end less grip compared to the mass it carries.

Table 31. Showing lateral weight transfer

	Down-force per wheel	Load inner [N]	Load outer [N]	Friction inner	Friction outer	Lat. F inner [N]	Lat. F outer [N]	Lateral acc. [m/s ²]	Speed [m/s ²]	Weight transfer [N]
1		1030,1	1030,1	1,608	1,608	1656,5	1656,5	15,78	11,02	831,5
2	68,0	266,5	1929,6	1,706	1,493	454,7	2880,9	15,88	11,06	837,2
3	68,5	261,3	1935,7	1,707	1,492	446,0	2888,5	15,88	11,06	836,9
4	68,4	261,6	1935,4	1,707	1,492	446,4	2888,1	15,88	11,06	836,9

When the final speed for the given turn has been found in the end of the iterations the time to complete a 180° turn with that radius is calculated.

Braking

Table 32. Input used for braking calculations

Wheelbase	1600 mm
CoG height	381 mm
Mass	350 kg
Downforce (at 20 m/s)	896 N
Drag (at 20 m/s)	679
Fraction of weight front	0.6
Tire friction coefficient	$1.74 - 1.28 \cdot 10^{-4} \cdot F_N$

The braking calculations are similar to those in Weight Transfer, the only difference is that the static weight is distributed according to the given fraction of weight front.

Table 33. Braking calculations

Iteration	Load per front [N]	Load per rear [N]	Friction front	Friction rear	Brake F per front [N]	Brake F per rear [N]	Brake acc. [m/s ²]	Weight transfer [N]
1	1253,95	910,60	1,579	1,623	1980,61	1478,31	19,77	1647,31
2	2077,60	86,95	1,474	1,729	3062,53	150,32	18,36	1530,12
3	2019,01	145,54	1,482	1,721	2991,30	250,53	18,52	1543,92
4	2025,91	138,64	1,481	1,722	2999,73	238,77	18,51	1542,34
5	2025,12	139,43	1,481	1,722	2998,77	240,12	18,51	1542,52

When the braking acceleration has been found in iteration 5, the drag is divided by the mass of the car and added to the acceleration.

The total braking acceleration is found for 4 different velocities; V_c , $V_c + 5$, $V_c + 10$ and $V_c + 15$ m/s where V_c is the cornering speed. Lagrange's Formula has been used to find a 3. polynomial giving the acceleration as a function of velocity. An example is shown below.

Table 34. Example of braking acceleration and corresponding velocities

Velocity, V	Acceleration, A	Time
26,06	-24,10	$t_i = 0$
21,06	-21,02	t_1
16,06	-18,55	t_2
11,06	-16,72	t_3

Table 34 show the values used to create the polynomial for $A(V)$.

	$A(V) = -16.72 \frac{(V - 16.06)(V - 21.06)(V - 26.06)}{(11.06 - 16.06)(11.06 - 21.06)(11.06 - 26.06)}$ $- 18.55 \frac{(V - 11.06)(V - 21.06)(V - 26.06)}{(16.06 - 11.06)(16.06 - 21.06)(16.06 - 26.06)}$ $- 21.02 \frac{(V - 16.06)(V - 16.06)(V - 26.06)}{(21.06 - 16.06)(21.06 - 16.06)(21.06 - 26.06)}$ $- 24.10 \frac{(V - 11.06)(V - 16.06)(V - 21.06)}{(26.06 - 11.06)(26.06 - 16.06)(26.06 - 21.06)}$	
	$A(V) = 4.144 * 10^{-5} * V^3 - 0.01479 * V^2 + 0.01227 * V - 15.108$	

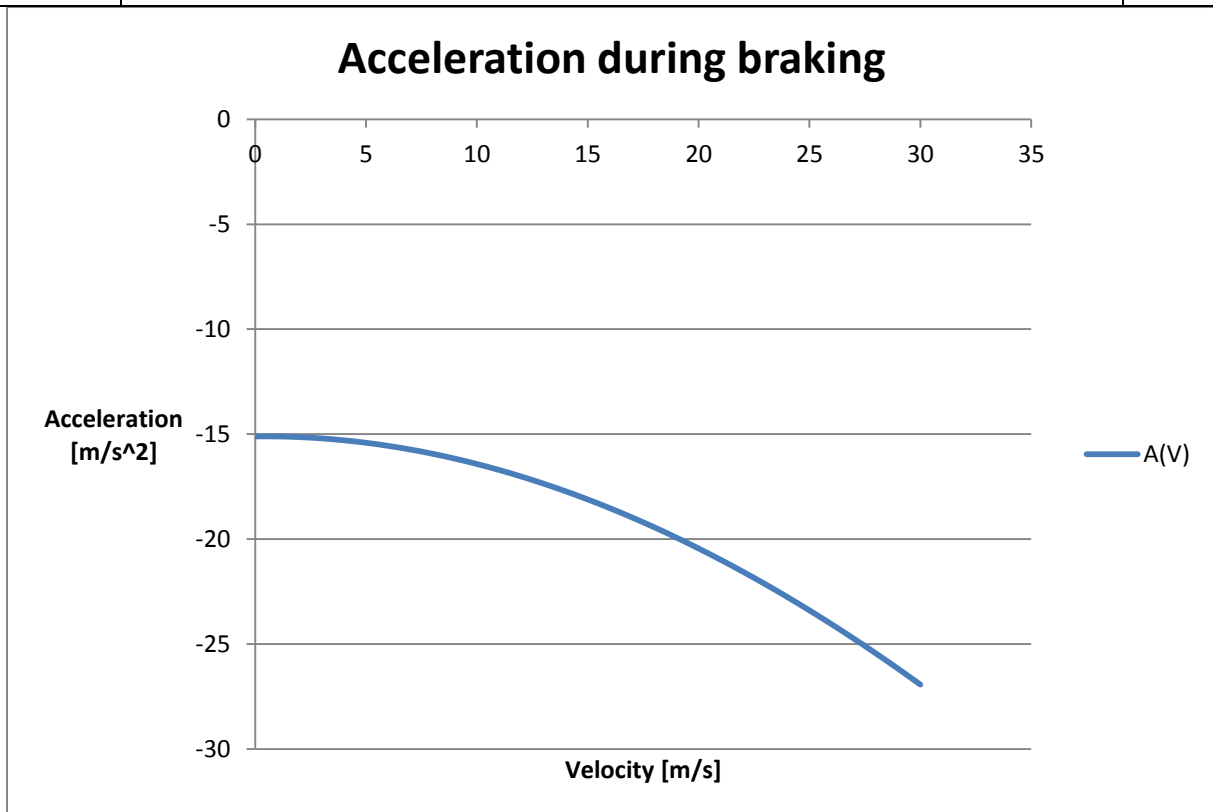


Figure 34. Plot of brake acceleration vs velocity

The plot for the polynomial seems reasonable since a nonlinear increase in absolute acceleration is expected due to aerodynamic drag and downforce. We have the acceleration as a function of velocity, need to find acceleration as a function of time. By integrating $A(V)$ in the velocity intervals and dividing by the velocity difference the average acceleration in the speed interval is found. The average acceleration is then divided by the velocity difference to find the time for each interval.

Finding average velocity between V_i and V_1	$\frac{\int_{V_i}^{V_1} A(V) dv}{V_1 - V_i} = \bar{A}$	
Finding time between V_i and V_1	$\frac{V_1 - V_i}{\bar{A}} = \Delta t$	

The steps above are repeated for all 3 velocity intervals. We now have 4 values of acceleration and 4 known times. A numeric example is shown below.

Table 35. Example values of velocity and acceleration

Velocity	Time	Acceleration
26.06	$t_i = 0$	-24.10
21.06	$t_1 = 0.222$	-21.02
16.06	$t_2 = 0.476$	-18.55
11.06	$t_3 = 0.760$	-16.72

Similarly as for acceleration and velocity we will now use Lagrange's Formula to find a 3. polynomial for $A(t)$. This polynomial is then integrated twice with respect to time to find position with respect to time, $x(t)$.

	$A(t) = 3.269 * t^3 - 10.92 * t^2 + 16.11 * t - 24.10$	
	$V(t) = 0.817 * t^4 - 3.64 * t^3 + 8.06 * t^2 - 24.10 * t + C1$	
C1 is V_i	$V(t) = 0.817 * t^4 - 3.64 * t^3 + 8.06 * t^2 - 24.10 * t + 26.06$	
	$x(t) = 0.163 * t^5 - 0.91 * t^4 + 2.69 * t^3 - 12.05 * t^2 + 26.06 * t + C2$	
C2 is initial position, set to zero	$x(t) = 0.163 * t^5 - 0.91 * t^4 + 2.69 * t^3 - 12.05 * t^2 + 26.06 * t$	

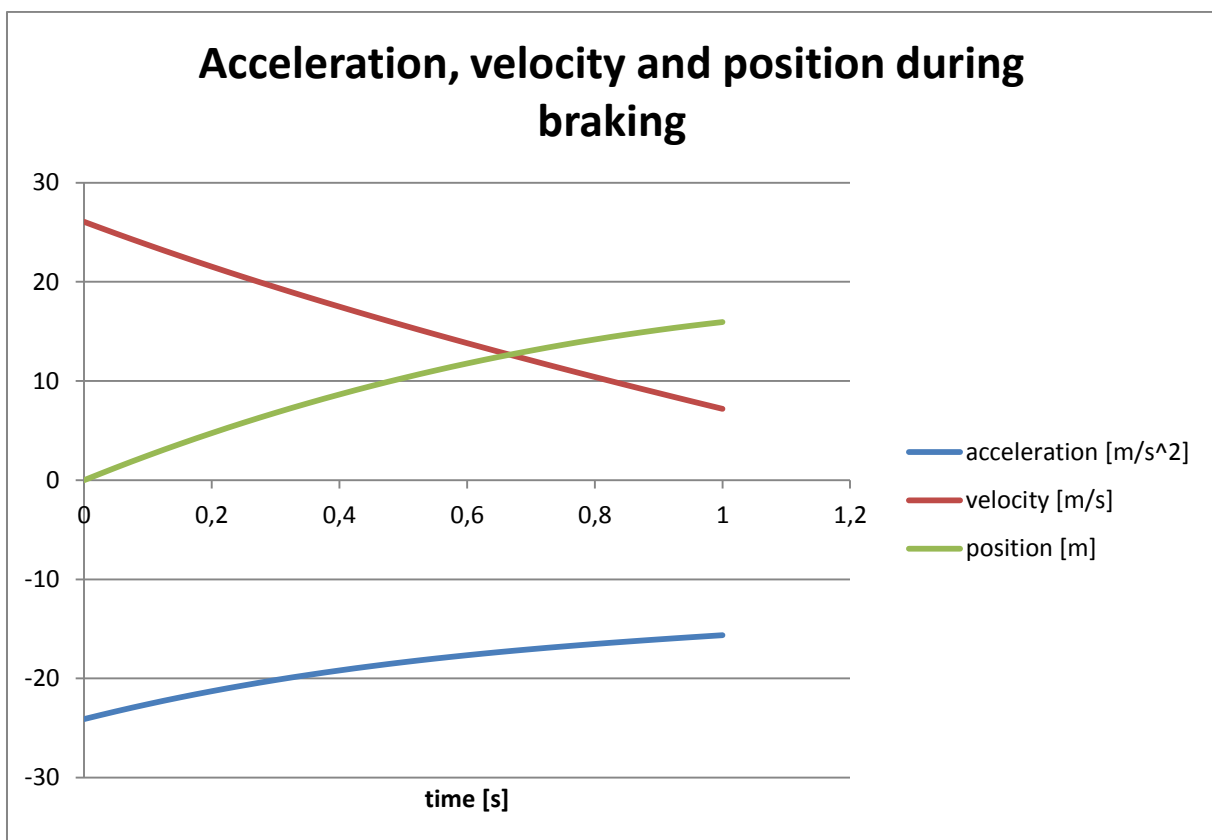


Figure 35. Acceleration, velocity and position vs time when braking

Acceleration

Acceleration is divided into two parts, grip-limited and power limited, similarly as in the Virtual Racetrack Setup. For both parts expressions for A(t), V(t) and x(t) are found the same way as for braking and therefor will not be shown.

Distributing the Straight Length

From the Virtual Racetrack Setup we have a 73 m straight. The maximum grip-limited acceleration is found in the intersection point between the A(V) curves for grip-limited and power-limited acceleration. A(V) for grip-limited acceleration is then used to determine the time to accelerate from the cornering speed to the maximum grip-limited speed. Using this time and x(t) the grip-limited distance is found.

We now have distance which must be distributed between power-limited acceleration and braking. Firstly, an acceleration time is guessed and a top speed is calculated based on this time. Secondly, an average acceleration when braking from top speed to cornering speed is found by:

	$\bar{A} = \frac{\int_{V_t}^{V_c} A(V) dV}{V_c - V_t}$	
	Where Vc and Vt is cornering and top speed respectively, A(V) is brake acceleration.	
Braking time, tb	$tb = \frac{V_c - V_t}{\bar{A}}$	
Braking distance as a function of time	$x(t) = \frac{\bar{A} * t^2}{2} + V_t * t$	
Inserting braking time	$x(tb) = \frac{\bar{A} * tb^2}{2} + V_t * tb$	

We now have the grip-limited, power-limited and braking distance but they will most likely not match the length of the straight. This is solved by calculating the distance deviation and the average speed for the power-limited and braking distance. The time required to move a distance corresponding to the deviation is calculated. Half of this time is then either added or subtracted from the initial a guess depending on whether the initial guess resulted in a too long or too short distance. This is repeated for 5 iteration loops in excel and the final values are used as the output for the Virtual Racetrack.